Extent and glacial history of the Cordilleran Ice Sheet in northwest Montana: Using OSL to date glacial sediments from the southeastern Flathead Lobe

by

Vidhesh Shukla

B.S., Barkatullah University, Bhopal, India, 2015
M.S., Barkatullah University, Bhopal, India, 2018

A THESIS

submitted in partial fulfillment of the requirements for the degree

MASTER OF SCIENCE

Department of Geology
College of Arts and Sciences

KANSAS STATE UNIVERSITY
Manhattan, Kansas

2023

Approved by:

Major Professor
Dr. Joel Spencer

Copyright

Abstract

This thesis investigates glacial sediments in the Flathead Valley, Polson, Montana that were deposited during the last glacial period (~115,000 – 11,700 years ago). Research objectives were to reconstruct the glacial history and timing of the furthest southeasterly extent of the Cordilleran Ice Sheet (CIS) at the Flathead Lobe in northwestern Montana and to assess the viability of luminescence dating of sediments in glacial environments.

The advance and retreat of past ice sheets can shed new light on our understanding of the cryosphere. The CIS was one of the major late Quaternary ice sheets. The CIS initially developed in southern Alaska but spread south during the Fraser Glaciation. The maximum extent of the CIS in the west is represented by the Juan de Fuca Lobe (17.5 ka) in Washington and in the east, it is represented by Flathead Lobe in Montana. The Flathead Lobe inhabited the Rocky Mountain Trench and terminated near the north end of the Mission Valley around Polson, Montana. The chronology of the western lobes of the CIS have received much attention, but not the easternmost lobes. There are only a few widely applicable and precise methods to date Quaternary landforms and sediments, and recent developments in optically stimulated luminescence (OSL) dating provide us with an opportunity to date a broad range of late Quaternary sediments. This thesis focused on the sedimentology and stratigraphy of surficial and older glacial sequences in the Flathead Valley and used OSL dating to establish age control for the deposits.

Fieldwork for the project was conducted during the summer of 2021, during which time the sites in the vicinity of Flathead Lake and Polson, Montana, representing Quaternary moraine deposits, glacial lake deposits, glacial lake outwash, and glacial till from localities consistent

with the position of the furthest extent of the Flathead Lobe were visited, described, and sampled. Updated digital elevation models were created to provide a comprehensive and detailed representation of the features associated with the terminal extent of the Flathead Lobe. Chronological constraints on the terminal extent of the CIS were obtained through small aliquot dating luminescence analysis of quartz from the glacial sediments. Ages from the Polson Moraine span from 15.0 ± 1.0 ka to 52.1 ± 2.9 ka, while those from the Elmo Moraine range from 45.4 ± 1.5 ka to 50.1 ± 1.5 ka.

This study used a combination of OSL geochronology, glacial geomorphology, and geospatial studies to determine the Polson Moraine of the Flathead Lobe as the maximum extent of the CIS. Seven samples were collected from various depositional environments to provide a comprehensive understanding of the glacial history and sedimentary processes that took place. Limitations to small-aliquot OSL dating of quartz sediments from the Polson and Elmo Moraine were encountered. These limitations were reflected in age overestimates except for Polson-03; limitations are most likely attributed to incomplete daylight bleaching of the quartz grains prior to deposition. Preliminary results from the Flathead Lobe suggest that bleaching potential of these glacial sediments is influenced by facies and depositional environment.

Table of Contents

List of Figures

List of Tables

Acknowledgements

I would like to express my sincere gratitude to my advisor, Dr. Joel Spencer, for his outstanding support and supervision throughout this project, from field work to lab work. Dr. Spencer's wisdom and approachable personality helped me develop my potential as a graduate student. His constructive feedback and valuable insights were instrumental in shaping my research.

I am also grateful to my committee members, Dr. Matthew Brueseke and Dr. Marc S. Hendrix, for their unwavering support, insightful feedback, and valuable expertise.

I am indebted to the KSU OSL Laboratory, KSU Geology Department, KSU College of Arts and Sciences, KSU Graduate Student Council, Geological Society of America, and Kansas Geological Foundation for their generous financial support towards research expenses, fieldwork, and conference attendance. This support was critical in facilitating the successful completion of this research.

Furthermore, I am grateful to Rick Van Voast, Chuck Forgey, Glacier Lake Sand and Gravel, and Treasure State Concrete for granting permission to conduct sampling on their property. Their cooperation was essential to the successful implementation of this research.

I owe a debt of gratitude to my late father, whose unwavering support, vision, and encouragement have always inspired me to overcome challenges in life.

Finally, I would like to express my appreciation to the Kansas State University Department of Geology, my peers, and my family for their continued support throughout my academic journey.

Chapter 1 - Introduction

1.1 Basement Geology

The Flathead region of northwest Montana lies within the Intermountain Seismic Belt (ISB), an area of active deformation and mountain building. The geological processes within this region are more complex than solely resulting from the collision of the North American and Pacific plates. Along with this collision, the subduction and collision of the Farallon plate have also played a crucial role in shaping the geology of the region. Furthermore, the geological characteristics of the ISB are not solely the result of collisional events. Much of the ISB, including the Flathead Valley, is characterized by extensional features, indicating that the region has undergone extension. This extensional nature post-dates the collisional events and must be incorporated into the overall understanding of the geological history of the region (Figure 1.1). The combination of these tectonic processes has not only influenced the uplift of the Rocky Mountains but also contributed to the formation of large structural features, such as the Lewis Overthrust, where older rocks are thrust over younger rocks.

Another major tectonic feature in the region is the north-south trending latest extensional Mission fault, a normal fault which is divided into two sections: the southern Mission Valley section and the northern Flathead Lake segment (LaPoint, 1971) (Figure 1.1). The extent and glacial history of the Cordilleran Ice Sheet (CIS) in northwestern America during the last glacial period has been influenced by the regional tectonic setting, specifically within the ISB where it advanced south from British Columbia flowing down the south-southeast trending Rocky Mountain trench (RMT) (Clark et al., 2009).

The study area in the Flathead Valley lies at the southern end of the northwest southeast striking RMT, a large intermontane valley in northwestern Montana extending ~1600 km into Canada (Fraser et al., 2021). Underlying fault systems along the length of the RMT have aided in its formation. The RMT has been divided into Northern Rocky Mountain Trench Fault that follows a major dextral strike slip system, and the southern portion that is characterized by extensional faults (Fraser et al., 2021). The Flathead Valley is bound by the Mission range on the east, the Salish Mountains in the west, and the Mission Valley to the south (Figure 1.1).

The basement geology of the region comprises rocks of the Proterozoic Belt Supergroup comprised of four major stratigraphic subdivisions: the lower Belt (~0-3 km), Ravali group (~3-5 km), Middle Belt Carbonate (~5-7 km) and Missoula Group (~7-10 km) (Mauk, 1983). These rocks, including quartzite, argillite, carbonates, and quartz arenite, were metamorphosed, and deformed during eastward thrusting and subsequent early- and mid- Cenozoic extension when the northwest southeast trending valleys were formed (Smith et al., 2004). During the late Tertiary (~23 - 2.5 million years ago) the Belt Supergroup sediments folded and faulted due to compressive forces from the collision of the North American plate with numerous large island arcs in the Pacific creating a zone of continuous structural disturbance along the length of US Cordillera known as the Sevier orogenic belt (Heller et al., 1986). The resulting mountain ranges were then eroded and extended along the RMT over millions of years, uncovering the rocks seen in the Flathead Valley today (Dickinson, 2004).

Figure 1.1 has been produced from a base map downloaded from Montana Bureau of Mines and Geology (Vuke et al., 2007). Different geological units have been color coded to identify them in the vicinity of the Flathead Valley. ArcGIS was used to overlay the Shuttle

Radar Topography Mission (SRTM) 1 Arc Second map of Polson on 1:500,000 geological map of Montana.

East of Salish mountains there is a thrust fault in the upper left corner of the map marked by sawteeth on upper plate symbol. There is a normal fault (identity and existence certain, location concealed) in the upper right corner of the map marked by ball and bar on downthrown block symbol. To the east there is a fault between the Flathead Lake and Mission Range. There is another normal fault (identity and existence certain, location concealed) that runs along the west side of the Flathead Lake and the down to the southern Polson Moraine. Quaternary glacial sediments in the study area are represented by Quaternary gravel deposits (Qgr) and Quaternary till deposits in the vicinity of Polson and Elmo moraine.

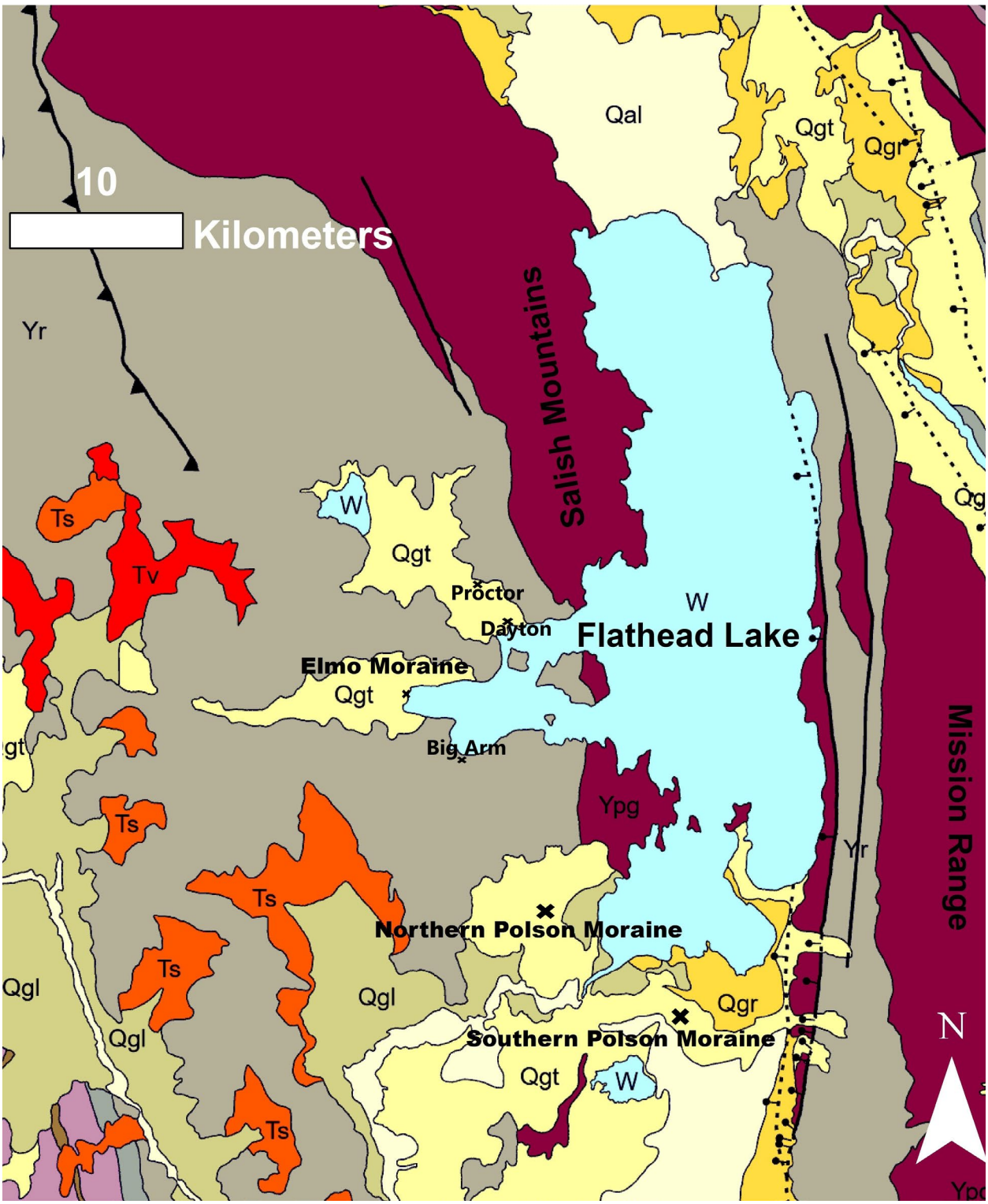

Figure 1.1: Geological Map of the Flathead region. Different geological units in the map are: Qgl – Quaternary Glacial Lake deposits, Qgr – Quaternary gravel deposits, Qgt: Quaternary glacial till, Qal – Quaternary Alluvium deposit, Ts – Tertiary sediment or sedimentary rock, Tv – Tertiary volcanic rock, Yr – Ravalli Group (St. Regis, Revett, and Burke Formations; or Empire

and Grinnell Formations; or Empire and Spokane Formations, Ypg – Piegan Group (Helena and Wallace Formations) and W – Water (Further map details in main text).

1.2 Quaternary Geology

Earth's climatic system over the last 2.6 million years has been affected by the growth and decay of continental ice sheets resulting in significant changes in global sea level. Careful reconstruction of the maximum extent of these ice sheets is imperative to provide controls for predicting future sea-level changes and to acknowledge their influence on various areas such as anthropology, long-term landscape evolution, paleoecology, genetic diversity, and glacial isostasy (Batchelor et al., 2019).

During the last glacial period, the North American Ice Sheet complex (NAICC) had a profound impact on the earth's cryosphere (Dyke et al., 2002). The NAICC consisted of four major ice sheets: the Cordilleran, Laurentide, Innuitian, and Greenland ice sheets (Lisiecki and Raymo, 2007) (Figure 1.2). These ice sheets had distinct formation times and physical and geographical characteristics (Cuffey & Marshall, 2000).

The CIS reached its maximum extent around 18,000 years ago (Dyke et al., 2002). As the youngest and smallest of the NAICC, the CIS covered an area of approximately 1.5 million km2 and extended from Alaska to the Rocky Mountains (Lisiecki and Raymo, 2007). The Laurentide Ice Sheet (LIS) reached its maximum extent around 26,000 years ago (Dyke et al., 2002). It was the oldest and largest of the NAICC, covering an area of approximately 10 million km2 and extending from the Arctic Ocean to the present-day Great Lakes region (Lisiecki and Raymo, 2007). The Innuit Ice sheet reached its maximum extent during the last glacial maximum of around 26,500 years ago (Dyke et al., 2002). This ice sheet covered a large portion of northern Canada, from the Canadian Arctic Islands to the southeastern part of the Hudson Bay, with an

area of approximately 2 million km^2 (Lisiecki and Raymo, 2007). The Greenland Ice Sheet reached its maximum extent of around 26,500 years ago (Dyke et al., 2002) and covered an area of approximately 2.7 million km^2, encompassing 85% of present-day Greenland (Cuffey & Marshall, 2000).

The Fraser glaciation was the last major glacial event in the Rocky Mountains of North America believed to have lasted from around 30,000 years to 10,000 years ago (Clark et al., 2009). During the late Pleistocene, the CIS started advancing south from British Columbia in low-lying mountain ranges and forming ice lobes in various mountain valleys (Carrara et al., 1986). The westernmost extent of the CIS was marked by the Juan de Fuca Lobe in Washington and along the east, the Flathead Lobe flowed through different mountain valleys and terminated in the Flathead Valley (Figure 1.1; 1.3) (Smith, 2004; Hendy, 2009; Hofmann and Hendrix, 2010).

For the entire Pleistocene glaciation (~2.6 - 0.012 million years), the upper Flathead River valley, the region above the present-day Flathead Lake, was filled with glacial ice (Alden, 1932; Locke, 1995). The Flathead Lobe flowed south-southeast down the Rocky Mountain Trench and merged with ice from the valley glaciers of the Galton, Whitefish, and Swan Ranges and terminated at the Polson Moraine, marking its maximum advance (Figure 1.4) (Smith, 2004). To the north of the Polson Moraine, Pleistocene sediments that include mostly till deposits represent glacial advance and retreat as the sediments were deposited by a combination of glacial meltwater and sediments formed from the ground-up rock and sediment that was transported by glaciers (Levish, 1997). To the south, Smith et al. (2004) note that the sediments in this area include Pleistocene deposits such as glacial outwash deposits, deposited by meltwater streams

flowing from the glaciers, as well as lacustrine sediments that were deposited in Glacial Lake Missoula (GLM).

Bedrock glacial striations indicate that near Big Arm, the Flathead Lobe split into two lobes, one lobe flowed south to Polson and the other one flowed west into the Big Arm, Elmo, and Dayton Valleys (Figure 1.4) (LaPoint, 1971; Bondurant, 2005; Edwards, 2006). A gentle north-plunging symmetrical anticline extends northwestward from Proctor, Montana through Lake Mary Ronan across the Flathead Lake and Elmo Quadrangles, this anticline is breached west of Elmo Valley by a steep-sided valley two to six miles wide called the Big Draw Valley. During the last glacial maximum, different sediments and moraines were deposited in the region around Flathead Lake, including the Elmo Moraine to the east (Bondurant, 2005; Johnson et al., 2014). It is possible that some of these deposits were submerged under GLM as the lake covered a large area of western Montana during the Pleistocene epoch.

The Polson Moraine (Figure 1.4) is oriented in the east-west direction and extends from the Mission mountains in the east to the west of Kerr Dam on the lower Flathead River (Johnson et al., 2014). The Polson Moraine is divided into southern and northern arms (Salmon, 2006). During the retreat of the ice, at the southern margin of the retreating ice sheet, a proglacial lake (occupying parts of modern Flathead Lake) was dammed by the terminal moraine (Polson Moraine) (Smith, 2004). The meltwater from the Flathead Lobe left a well-preserved record of varying hydrology with deglaciation (Hofmann and Hendrix, 2010).

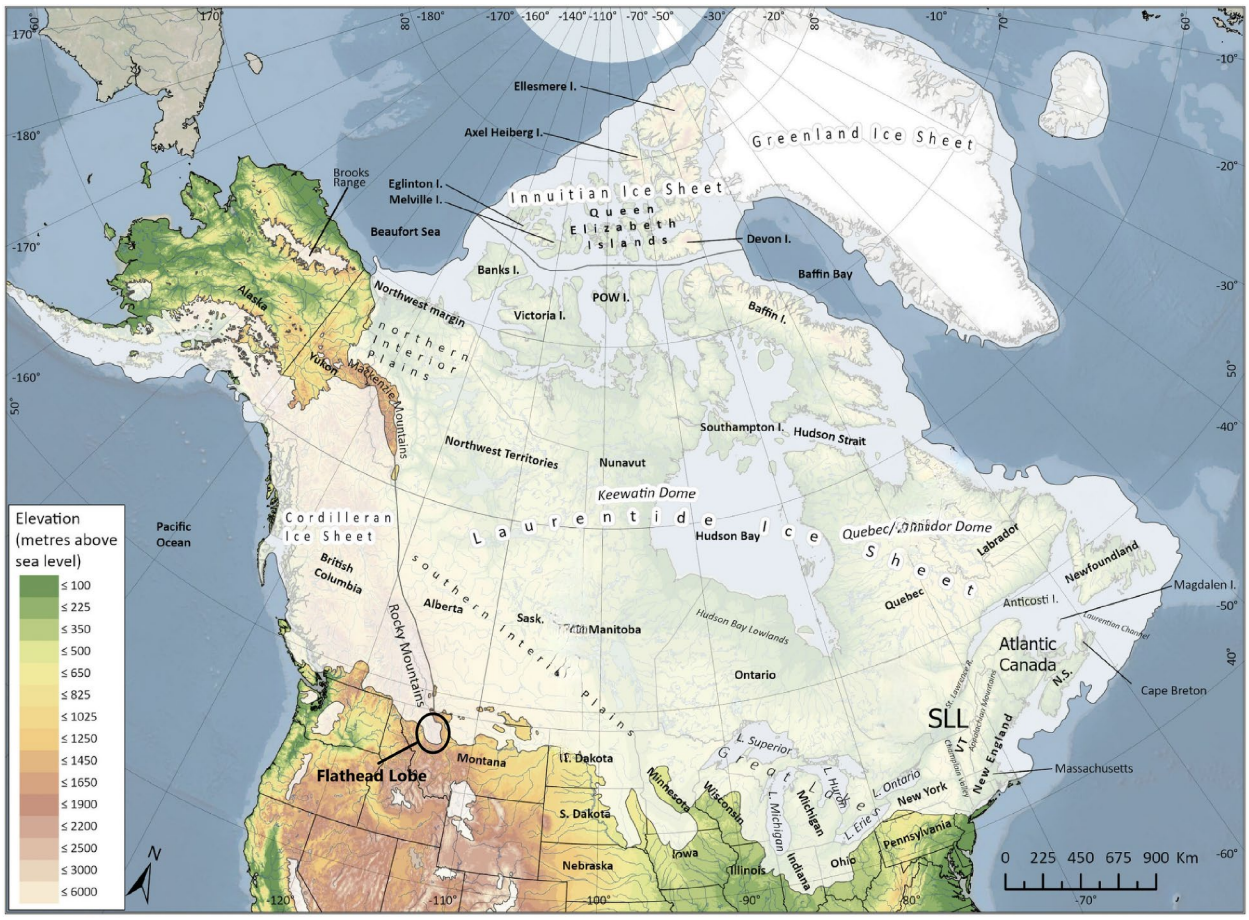

Figure 1.2: This figure depicts the extent of ice coverage in North America during the Last Glacial Maximum, showing the Laurentide, Cordilleran, Innuitian, and Greenland ice sheets (from Dalton et al., 2020). The circle highlights the study area: the Flathead Lobe, which represents the maximum extent of the CIS in northwest Montana.

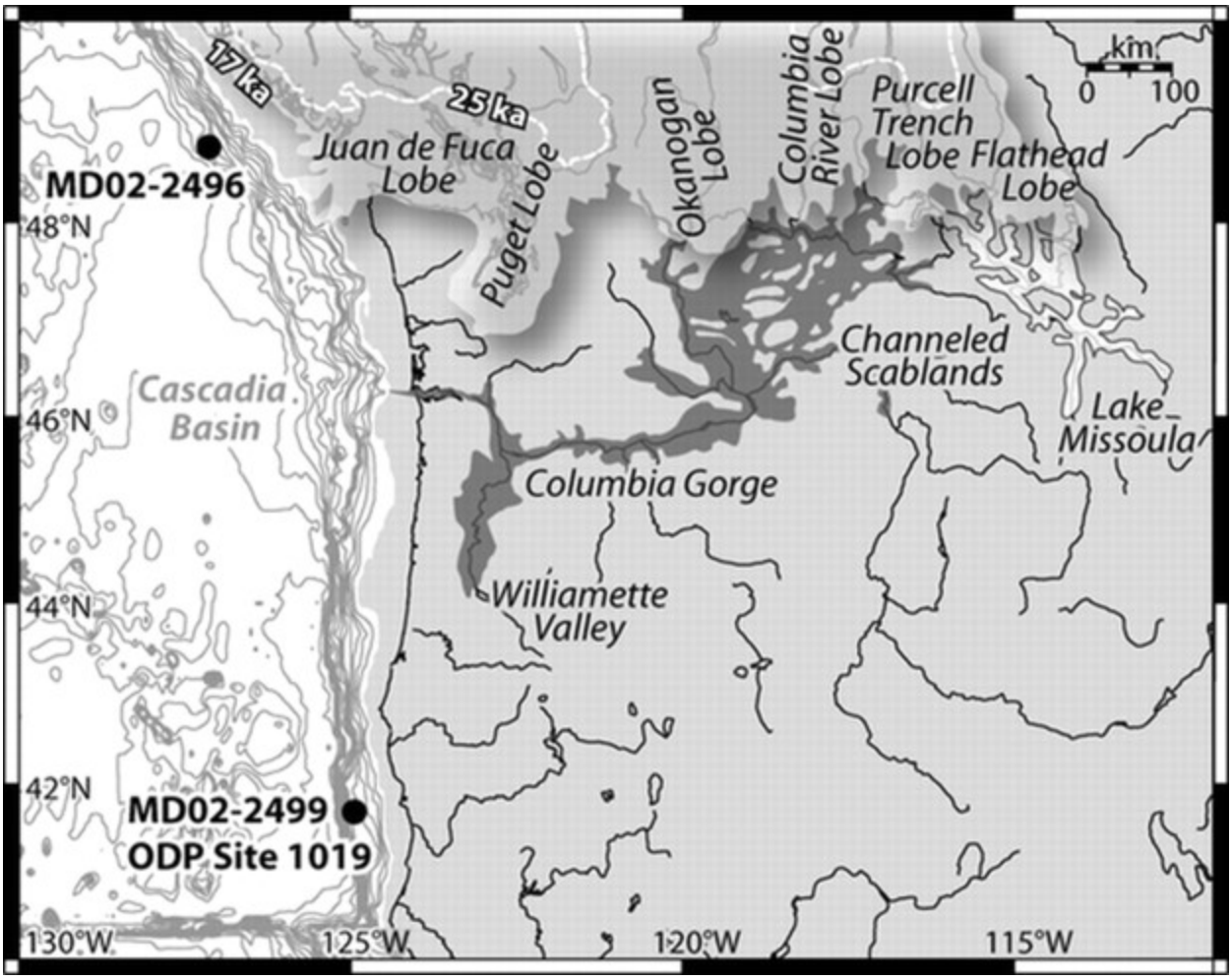

Figure 1.3: Map of northwestern American margin showing location of the southern lobes of the Cordilleran Ice Sheet. The maximum extent of the Cordilleran Ice Sheet at 25 ka (heavy dashed white line) and at 17 ka (3-dimensional white shading) is indicated (from Hendy 2009).

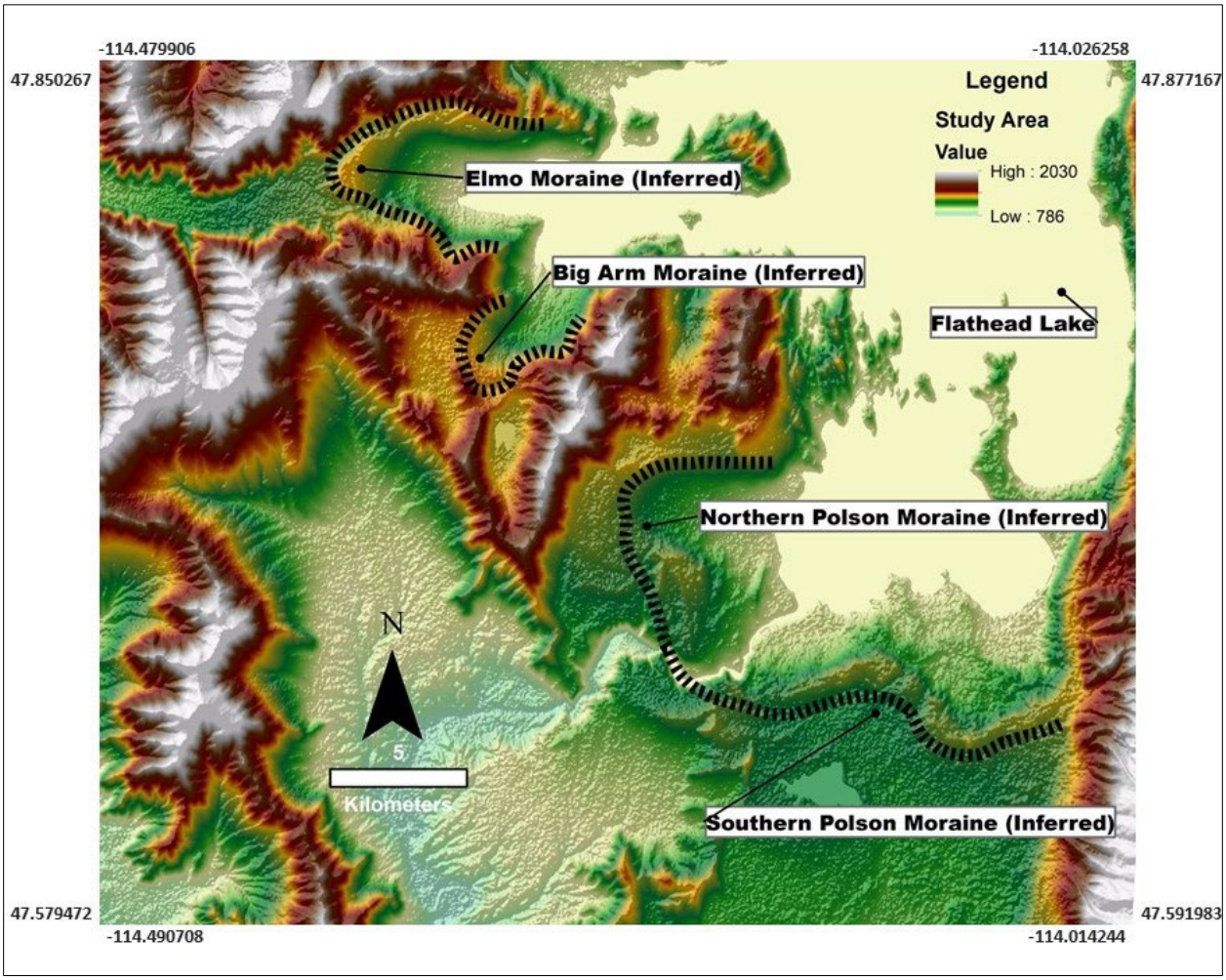

Figure 1.4: Digital elevation model of the study area depicting the maximum extent of the Flathead Lobe with the terminal moraine as the Polson Moraine and the lateral moraine as the Elmo Moraine. The moraine can be seen elevated as an arcuate ridge marked by southern and northern Polson Moraine. The section of Elmo Moraine is also identified by an elevated ridge at the same elevations as the Polson Moraine.

1.3 Geochronology

Although there have been no direct dating studies to determine the depositional age of the Polson Moraine, there have been several dating studies that help us determine the constraint on the likely age of the maximum extent of the Flathead Lobe. Past studies have attempted to investigate the glacial history of the Flathead Lobe by utilizing the descriptive logs of borehole

cuttings to interpret stratigraphy and sedimentology to the north of the Polson Moraine, in the Flathead Valley (Smith, 2004). Levish (1997) suggested that the age of the Polson Moraine is related to the draining of GLM and is temporally similar. Smith et al. (2000) speculate that the central part of the Polson Moraine was deposited somewhere between 19 and 15 ka, the time of the last glacial maximum in the area. Studies by (Mudge 1967; Carrara, 1986) found the presence of Glacier Peak ash (G ash) in a postglacial alluvial fan at the Sun River Canyon along the continental divide of Montana, located ~100 km east of the Flathead Lake. The ash occurs as a 3 cm thick white lens in this unit, along with shells of molluscs that were radiocarbon dated at 12,750 ± 350 BP. Another study, using radiocarbon dating on a pine needle in a rhythmite section from the core of the central basin of Flathead Lake, gave an age of 14,150 ± 50 cal yr BP for the glacial retreat (Hofmann et al., 2006).

Levish (1997) used a combination of optically stimulated luminescence (OSL), thermoluminescence, and radiocarbon dating on glacial lacustrine sediments ~36 km to the south of the Polson Moraine at the Bison Range section, Mission Valley. Outwash from the Flathead Lobe, both south of Polson and west of the town of Elmo, MT is not overlain by lake sediment suggesting that outwash is younger than the lake sediment and the Flathead Lobe was near its terminal position (Levish 1997). The OSL age of GLM, suggests that the lake filled the valley from about 19.2 to 16 ka (Levish 1997).

GLM was a proglacial lake formed due to repeated ice damming that overflowed and released huge volumes of water, which led to the deposition of rhythmites in the area. An OSL study on rhythmites along the rail line section ~90 km to the south, and Ninemile section ~78 km to the southwest, of the Polson Moraine, yielded ages of 13.7 ± 0.5 ka to 12.4 ± 0.5 ka in the rail

line section and 15.1 ± 0.6 ka to 13.6 ± 0.6 ka in the Ninemile section for the GLM flooding (Hanson et al., 2012).

Bondurant (2005) studied the sedimentology of deposits in the Big Arm, Elmo and the Proctor area and established cross-cutting relationships between features in the Flathead Valley. Well logs in the Flathead Valley were analyzed using individual observations and descriptions from Smith (2004). Active gravel pits, road cuts in the Elmo moraine, and active drainage in the Proctor/Dayton Valleys were measured, and the last composition was determined at various elevations to define provenance and ice sheet elevations, revealing the formation of the Proctor, Elmo, and Big Arm Moraines to be between ~25,000-12,300 years BP (Bondurant, 2005).

Another OSL dating study on glaciolacustrine sediments within the GLM impoundment in the Garden Gulch area ~130 km southeast of Polson gave an OSL age of 20.9 ± 1.3 ka (Smith et al., 2018). Lastly, proglacial sediments at Dayton Creek Delta described by Bondurant (2005) indicate proximity to the westward arm of the Flathead Lobe ice margin. A series of delta foresets from the Dayton Creek Delta were analyzed in an earlier project at Kansas State University and gave preliminary OSL ages of 18.6 to 24.3 ka (Spencer & Spencer, 2019).

The geochronological studies above provide deglaciation ages for the Flathead Lobe, draining of the Glacial Lake Missoula. Despite the various chronological studies conducted in the Flathead Valley region and to the south of the Flathead Lake, an accurate age for the maximum extent of the Flathead Lobe remains unclear.

1.4 This Study

This study uses the OSL dating technique to attempt to constrain the age of the past glacial features associated with the terminal moraine of the Flathead Lobe. In the southerly

reaches of the CIS, the age of the maximum extent of the western lobes is well constrained, but not the easternmost lobes (Hendy, 2009). Past, studies have inferred pre-last-glacial-maximum till to be present south of the Polson Moraine in the Mission and Jocko Valleys (Stoffel, 1980). However, sedimentology-based studies in the Mission Valley could not attribute any deposits or geomorphological features related to the Flathead Lobe beyond the Polson Moraine (Smith, 2004). As highlighted by Smith (2004), due to the lack of dates from the glacial deposits near the Polson Moraine, details of the timing of the glacial maximum of the Flathead Lobe are still unclear.

This study attempts to refine the glacial chronology of the Flathead Lobe at the southeastern extent of the CIS. The hypothesis proposed is that the age of the eastern lobes of the CIS should be comparable to that of the well-constrained chronology of the western CIS. This will involve an examination of the geological evidence, including glacial landforms, sediments, and geochronological data, to establish a robust chronology for this lobe and to compare it with the chronology of the western CIS. New chronological data will be obtained using OSL techniques—in combination with any available independent dating evidence—and obtained ages compared with the age of the westernmost CIS.

Given the challenge to OSL methods of sediments in ice-proximal settings (see Section 3.2.1), objectives are to determine the depositional ages of glacial sediments in the study area using small aliquot OSL analysis. Studies that have used OSL dating to glacial deposits note that in glaciofluvial, glaciolacustrine, and glaciomarine depositional environments partial resetting (bleaching) of the apparent dose at the time of deposition can lead to the overestimation of burial ages (King et al., 2014; Fuchs and Owen, 2008). The partial resetting occurs because these sedimentary environments can result in limited light exposure of sediment grains during

transport, where they are transported rapidly, and over short distances, such as in a turbulent meltwater flow. Another challenge for insufficient bleaching could be transportation/deposition during hours of darkness resulting in a heterogeneous mixture of partially bleached and well bleached samples (Thrasher et al., 2009). Several studies have shown that glacially driven sediments have poor quartz luminescence sensitivity because of the geologically young bedrock sources, a lack of subaerial weathering of grains or an insufficient number of bleaching and dosing cycles prior to deposition (Spencer and Owen, 2004; Lukas et al., 2007; Thrasher et al., 2009).

To accurately quantify luminescence properties the sedimentology and specific depositional setting must be characterized for appropriate sample selection. Comparing data from quartz obtained, past geochronological studies and examination of geological studies, the study will provide a more robust understanding of the depositional history in the study area, providing insights into its glacial history and depositional processes.

Chapter 2 - Study area and Sampling sites

The sampling sites were chosen based on past studies which determined the maximum extent of the Cordilleran Ice Sheet in NW Montana as the Flathead Lobe. The Polson Moraine is the terminal moraine of the Flathead Lobe (Hofmann and Hendrix, 2010). The Polson Moraine forms a hilly belt extending from one to three km in width, it extends in a crescent shape approximately eight to ten miles west from the Mission range (Davis, 1920).

The Polson Moraine in Montana (Figure 1.4), which is bisected by the Flathead River and stretches from the Mission Mountains to Kerr Dam, is a topographical expression of the former terminus of the Flathead Ice Lobe (Hofmann et al., 2006). The formation of this moraine can be understood through the glaciofluvial delta model, also referred to as the outwash fan or sandur delta (Lønne, 1995).

The southern and northern parts of the Polson Moraine display dissimilar sedimentological and structural traits. The southern segment of the moraine starts at the shore of Flathead Lake and reaches the southern edge of Pablo Reservoir (Braden, 2006). Samples Polson-03, Polson-06, and Polson-07 were collected from this area (Figure 2.1). The abundance of climbing current ripples found in the Redi-Mix gravel pit along US Highway 93 (Hofmann et al., 2006) suggests that this part of the moraine was formed under subaqueous conditions. The dominant facies in the southern segment of the moraine are Gcm (clast-supported, massive gravel) and Gmm (matrix-supported, massive gravel), with occasional interbedding of Gmf (massive matrix-supported gravel, fine) facies (Braden, 2006). The Polson-06 and Polson-07 samples obtained from a quarry located on the southern arm of the moraine show a mixture of scattered gravel and laminated beds.

The northern part of the Polson Moraine is located west of Polson and north of the Flathead River (Figure 2.1) (Braden, 2006). Samples Polson-01 and Polson-02 were collected from this area. This section of the moraine is primarily composed of the Gmf facies and is thought to have been deposited in a subaerial (terrestrial) environment shaped by shallow bedrock and lacking any structural or flow direction (Smith, 2004). However, a roadcut measured section along Irvine Flats Road was found to be composed of sediment consisting of laminated and thinly bedded (1 cm) brown clay and silt, as well as thin beds of fine to very fine tan sand (Braden, 2006). This study also discovered the presence of three distinct layers of reddish-brown silt with small pebbles on top of the layer within the clay and silt beds, as well as wavy clay and sand layers truncated by a bed of reddish-brown silt. The Polson-02 sample obtained from laminated beds indicates a low energy depositional environment (Hofmann et al., 2006).

The Elmo Moraine, as reported by Bondurant (2005), was formed in a subaqueous environment when the portion of the Flathead Lobe flowed into the Big Arm Embayment and terminated into GLM. Samples Elmo-04 and Elmo-05 were taken from a roadcut along Montana Highway 28 and are composed of poorly sorted sands and gravel (Lønne, 1995). Bondurant (2005) also identified two sets of fluvial channels extending from the Elmo Moraine towards the west, with the first channel set believed to have been created by flow from supraglacial waters when the ice lobe was in its terminal position.

In this study, the Polson Moraine was explored as a key site in understanding the past glacial history of the Flathead Lobe of the CIS in Montana. The Polson Moraine exhibits a mix of subaqueous deltaic and fluvial-style deposition as well as subaerial deposits and provides valuable insights into the glacial history of the region. The samples were collected from various

depositional environments including Quaternary till deposit (Qgt), Quaternary glacial lake deposits (Qgl), and Quaternary alluvium (Qal) deposits. The sample descriptions included information on the depositional environment, sediment characteristics, and overburden of each sampling site. Digital elevation models (DEMs) were created to observe the topography of the Polson and Elmo Moraine (Section 3.1.1). Figure 2.1 is a Google Earth™ image of the sampling sites in the study area.

Figure 2.1: Google Earth™ image of the study area indicating sampling sites from both the Polson Moraine and the Elmo Moraine.

2.1 Sampling Sites and sample descriptions

Samples were collected from seven sites (Figure 2.1). Five from the Polson Moraine, POL- 071221-01, POL-071221-02, POL071221-03, POL071321-06, and POL071321-07, hereafter referred to as Polson-01, Polson-02, Polson-03, Polson-06, and Polson-07, respectively,

and two from the Elmo Moraine, ELMO-071321-04 and ELMO-071321-05, hereafter Elmo-04 and Elmo-05, respectively.

2.1.1 Polson-01 (47°41'21.93"N 114°14'14.31"W)

The sampling site is a part of the Quaternary till deposit (Qgt) (Vuke et al., 2007) (Figure 2.2). It is a section of the western extent of the Polson Moraine, the exposed section has a length of ~57 m and a height of ~2 m and is a part of the northern Polson Moraine (Salmon, 2006). The sediments are matrix-supported with clasts (mostly pebble-sized) ranging from ~1-10 cm. The samples were collected from the portion of the moraine where laminated beds are exposed as they likely represent the original depositional environment, confirm there is no observable post-depositional disturbance, and hence can provide more accurate ages when dated using OSL dating. The overburden was ~2 m excluding the topsoil; the topsoil is a much later addition to the overburden depth and therefore was not considered in estimates of cosmogenic dose over the burial period of the sample. The sample that was collected had light-colored fine silt to sand-sized grains with medium-sized clasts of ~0.5-1.5 cm.

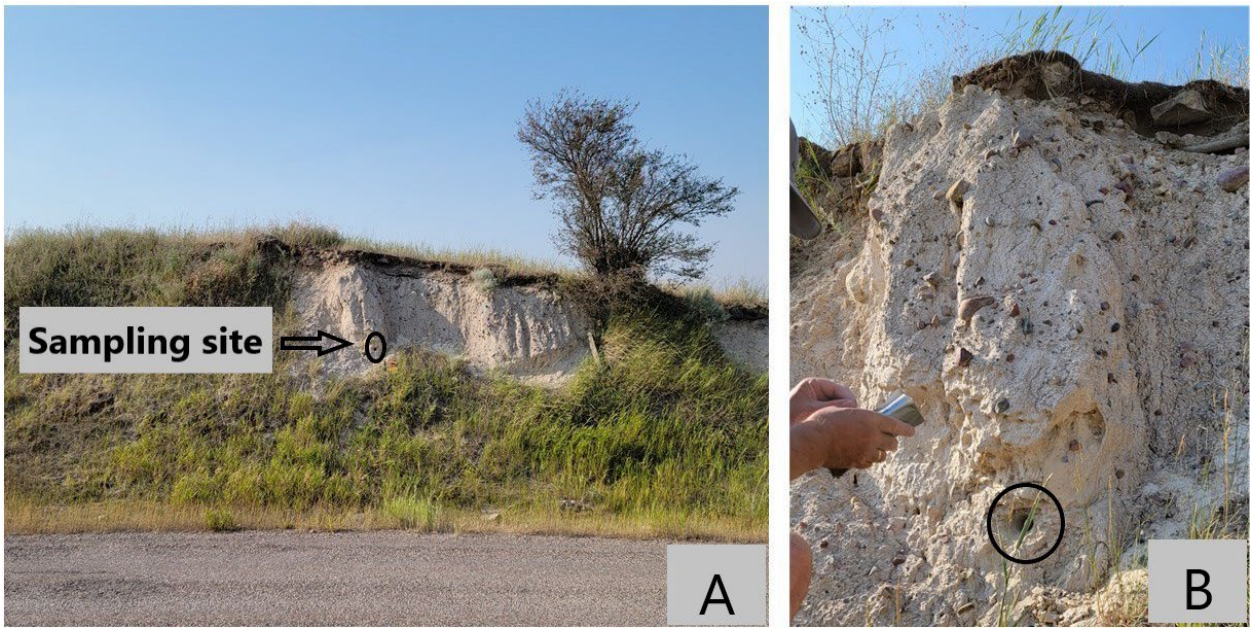

Figure 2.2: Polson-01. Glacial till (Qgt) exposed in a roadcut. The circle on both A & B indicates the sampling point. Image B is a close-up shot of the sampling point.

2.1.2 Polson-02 (47°40'42.82"N 114°16'58.61"W)

This sampling site was located further to the west compared to Polson-01 and is a part of northern Polson Moraine (Salmon, 2006) (Figure 2.3). These are mapped as Quaternary glacial lake deposits (Qgl) – containing light brown laminated silt, fine grain sand, and clay (Vuke et al., 2007). The sediments are matrix-supported. There are a series of laminations ~1-2 cm in thickness present throughout the outcrop. Erosion and weathering of these deposits has resulted in hoodoo-like features. The overburden on the sampling site is ~4.5 m. The presence of laminated beds is indicative of a low energy depositional environment, and sample Polson-02 was collected from these laminated beds. Fine-grained silt sized clasts were observed in the sample.

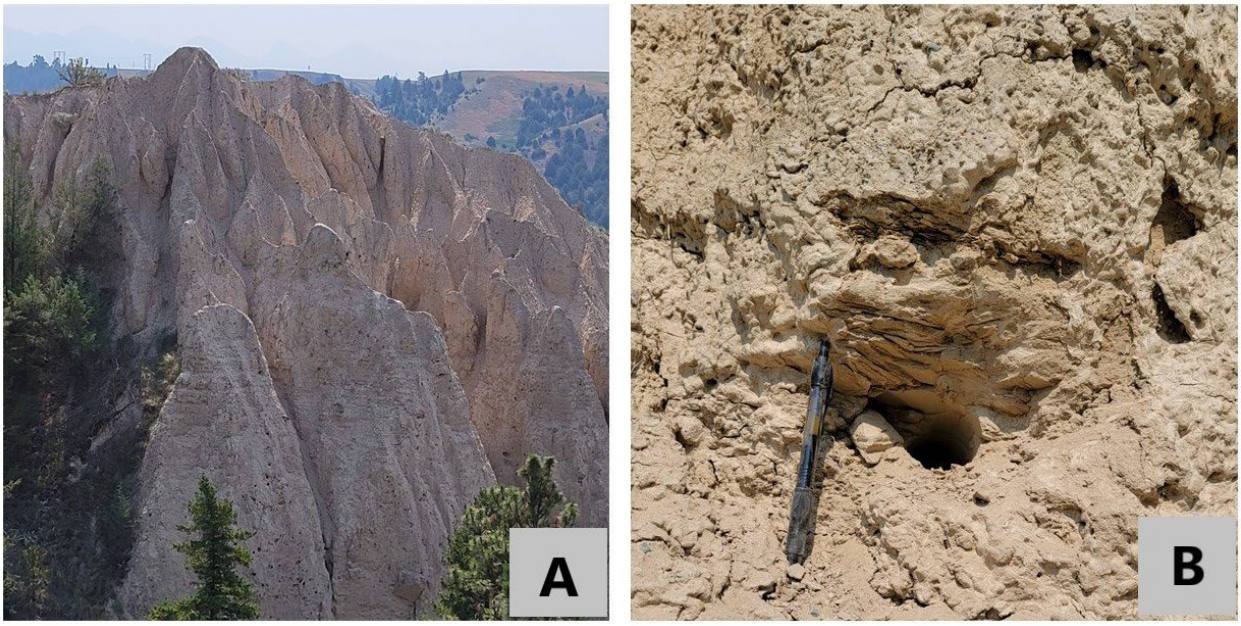

Figure 2.3: Polson-02. Image A shows the prominent hoodoo-like features identified as ice proximal deposits (Vuke et al., 2007). Image B is the sampling location with visible bedding structures.

2.1.3 Polson-03 (47°38'27.69"N 114° 7'42.46"W)

The sampling site is a Quaternary alluvium (Qal) deposit and contains sand, silt, and clay deposits of streams and river channels, and floodplains (Vuke et al., 2007). It was collected immediately south of the southern Polson Moraine (Salmon, 2006) (Figure 2.4), with the goal of helping us identify the southernmost extent of the Polson Moraine. The sample was collected from the Treasure State Concrete sand and gravel quarry. Well-sorted sand-sized grains (Table 3) were observed in the sample.

Figure 2.4: Polson-03, the circle indicates the sampling location.

2.1.4 Elmo-04 (47°49'14.30"N 114°23'30.10"W) & Elmo-05 (47°49'13.10"N 114°23'30.60"W):

The sampling site is at a locality where a part of Flathead Lobe split and flowed to the west (Figure 2.5) and glacial sediments were deposited in the Elmo Valley. The sampling site is exposed in a roadcut of Montana Highway 28. It is mapped as a Quaternary glacial till (Qgt) (Vuke et al., 2007) deposit mainly composed of poorly sorted sands and gravel. The samples were collected from a fine sand deposit with ~0.5-1 cm thick laminated beds. The overburden above the sampling position was ~2 m.

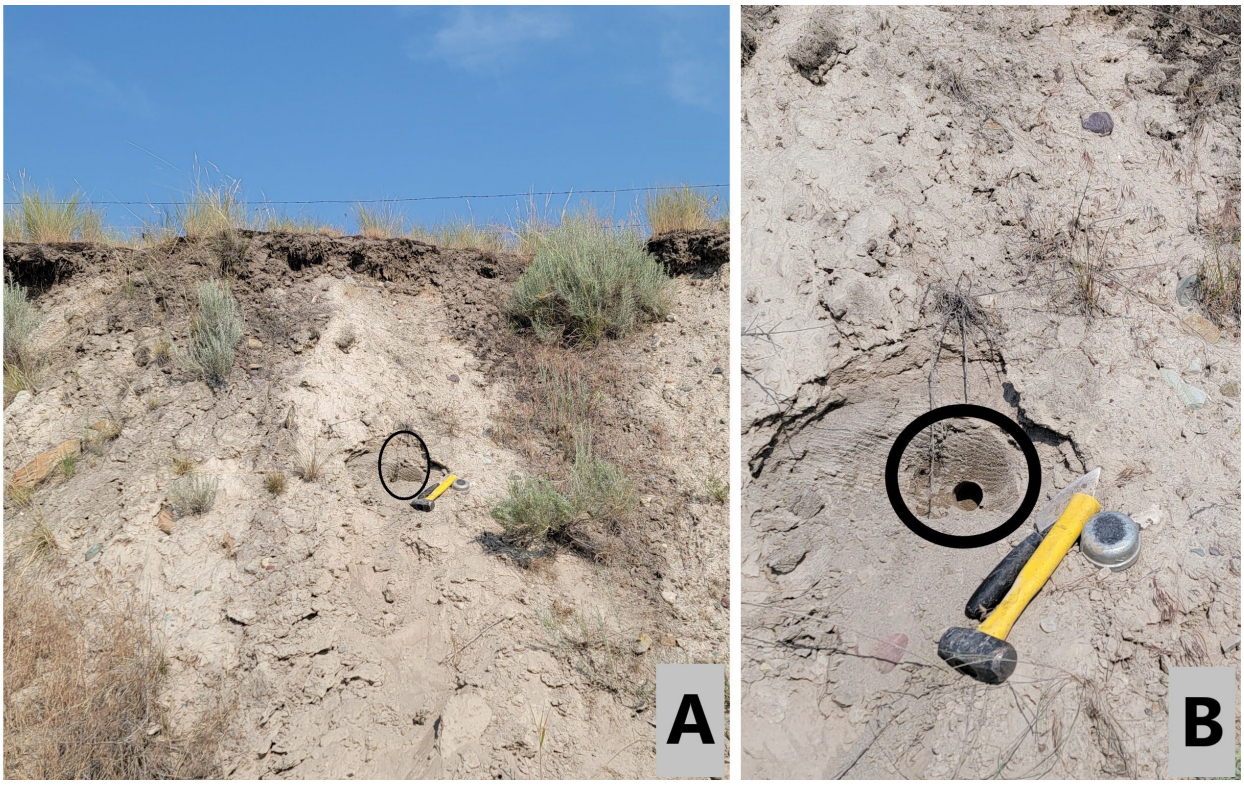

Figure 2.5: Elmo-04 and Elmo-05. Sampling location of Elmo-05 (not shown) was collected from the same feature ~30 m along the exposure to the southwest. Black circle in A and B indicates sampling position for Elmo-04; close up in B shows the laminated beds where the sample was collected.

2.1.5 Polson-06 (47°39'48.40"N 114° 8'40.00"W) & Polson-07 (47°39'46.80"N 114° 8'42.10"W):

The sampling site is in the southern part of the Polson Moraine (Figure 2.6). Even though the deposits are mapped as Quaternary glacial lake deposits (Qgl) (Vuke et al., 2007), there is also a glacial-fluvial input at this location. The sampling site is at the Glacier Lake Sand and Gravel quarry located on the southern arm of the Polson Moraine. Polson-06 was sampled from the top of the depositional setting, with outcropping sandy laminated beds. Polson-07 was sampled from the bottom of the exposure in a series of basal laminated beds.

The southern arm of the Polson Moraine where these samples were collected is believed to have formed in subaqueous conditions (Hofmann et al., 2006). The sampling site contains gravel mixed with laminated beds. A series of laminated beds are present at the top of the deposit, with gravel units at the bottom. The samples were collected from the laminated beds. The presence of gravel suggests periods of higher energy deposition, such as during glacio-fluvial activity. Alternating laminated beds and gravel could indicate alternating subaqueous and glacio-fluvial depositional environments.

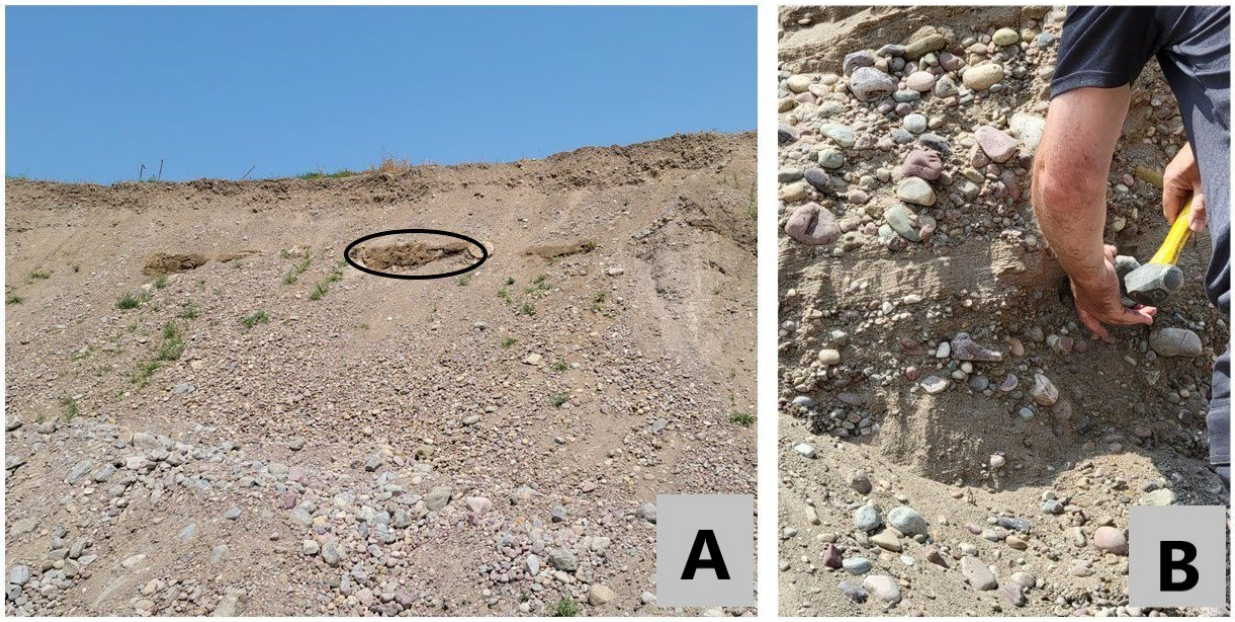

Figure 2.6: Polson-06 and Polson-07 sampling sites are from the same quarry representing the top and bottom of the depositional settings. A) shows an overview of the working face of the quarry with the Polson-06 sampling locality with outcropping sandy laminated beds indicated with the black oval. B) shows a layer of basal laminated beds with pebbly-cobbly units above and below. Polson-07 was collected from the basal laminated beds.

Chapter 3 - Methodology and results

3.1 Landscape Analysis

3.1.1 DEM model (Figure 1.4)

A DEM was generated for the study region in ArcGIS by acquiring data, preprocessing the data, creating a terrain dataset, importing data, building pyramids, generating the DEM, editing it, and validating its accuracy. Required data was obtained to generate the DEM, which included digital orthophoto quadrangles (DOQs) - digital aerial photographs of the study region, and digital elevation data that is 1 arc-second DEM that covers an area of approximately 30 m x 30 m. The data was preprocessed to ensure that it was in a format that could be used to generate the DEM. This involved converting data formats, re-projecting data to a common coordinate system, and ensuring that the data was free of errors or anomalies. Terrain Dataset was created using the ArcGIS Spatial Analyst extension. Digital elevation data and DOQs were imported into the Terrain Dataset. The DEM was edited as required to remove any errors or anomalies, using the "Terrain Editing" tools available in the toolbox.

Figure 1.4 is the DEM model, where the model color codes the high, low, and intermediate elevation values with detailed visualization of the terrain. The model can be used to observe past erosion and sedimentation in the region. The model can also be used to show the extent of glacial activity and the morphology of glacial landforms. It is clearly visible from the model that there is an abrupt rise in the elevation near the northern and southern Polson Moraine and the Elmo Moraine. The Polson and Elmo Moraines can be marked as an arcuate ridge indicated by the inferred limit of the moraines on Figure 1.4. Based on the color coding it can be observed that the northern and southern Polson Moraines lie at the same elevation, implying that

they are a part of the terminal extent of the Flathead Lobe in the region. The Elmo Moraine can also be observed at the same elevation level as the Polson Moraine. The model can be compared to earlier work in the region, and the generated DEM provides a more comprehensive and detailed representation of the topography in the study area, incorporating both DOQs and digital elevation data.

3.1.2 Contour Map (Figure 3.1)

Moraines are deposits of glacial debris, including rock, very little amount of soil, and ice, which are left behind by an ice sheet when it is stationary for some time. These deposits can cause changes in elevation and topography, which can be detected on a map by evaluating contour lines. On the contour map (Figure 3.1), it can be observed that the Polson and Elmo Moraines generally lie on the ~1000 m contour line. The contour map also highlights the presence of ridges, valleys, and other landforms that have been shaped by glacial activity. The contour map helps to identify the elevation and slope of the moraines, which allows for the understanding of the behavior of the glacier and its impact on the landscape. The “Contours” tool in ArcGIS was used to overlay the contour map on the DEM model.

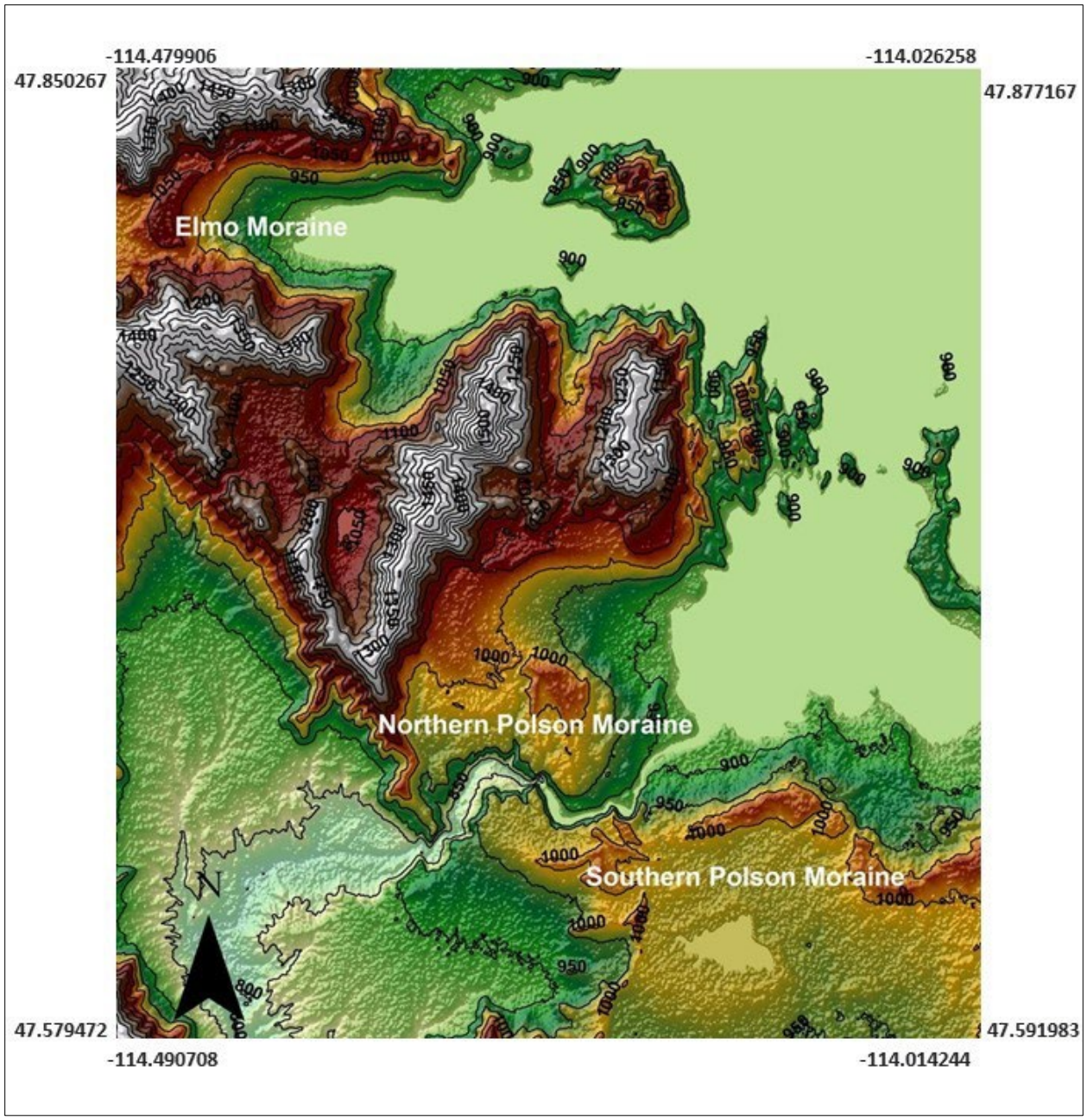

Figure 3.1: Contour map showing differences in elevation (in meters). There is a sudden rise in elevation of ~60 m where the moraines were deposited.

3.2 OSL Methods and Results

3.2.1 OSL background

Optically stimulated luminescence dating is widely used to determine the time elapsed since the last exposure of geologically young sediments to sunlight. The method involves four steps: (1) Exposure to natural daylight resets prior trapped charge within mineral grains (e.g., usually quartz or alkali feldspar), (2) charge accumulates and is trapped in the buried grains due to ionizing environmental radiation, (3) sample is collected and trapped OSL charge concentration is measured, and (4) at each location the environmental dose rate grains are subjected to is measured (Rhodes, 2011) (Figure 1.4). Minerals trap the charge as they have lattice-charge defects formed during crystallization and from subsequent exposure to ionizing radiation. The concentration of trapped charge is evaluated by laboratory OSL measurements. The single-aliquot regenerative-dose (SAR) protocol of Murray and Wintle (2000, 2003), is an accurate and reliable protocol and it is applied for OSL age estimates (Rittenour, 2008; Rhodes, 2011).

The environmental dose rate (measured in Gy/ka), which is an estimate of the exposure of mineral grains to ionizing radiation from the decay of U and Th series, 40K, and cosmic sources during the burial period, can be determined by geochemical analyses (Duller, 2012).

$$age \; = \; equivalent\; dose \frac{De}{environmental} dose\; rate\; (Dr),$$

[ka = Gy/(Gy/ka)]

where the equivalent dose (De, measured in grays (Gy), 1 Gy = 1 J/Kg) is equivalent to the radiation energy absorbed and trapped in the sample since the relevant OSL traps were last emptied. The environmental dose rate (Dr) corresponds to the rate at which dose is deposited by

ionizing radiation from natural radioactivity from the sample mineral grains, the sedimentary burial environmental, and from cosmogenic radiation.

In the OSL lab, the light sensitive traps in quartz and feldspar are sampled by stimulating the grains using blue or green photons while for feldspar near-infrared (NIR) light, and the resulting UV emissions are counted to estimate the equivalent dose (De) (Wintle and Murray, 2006). It is important to note that the emission spectrum of quartz can vary, and the type of excitation used and the presence of impurities in the sample can impact its emission spectrum (Krbetschek et al., 1997). Quartz is typically known to emit ultraviolet (UV) light (Krbetschek et al., 1997), but it can also emit light in other wavelength bands such as visible light and near-infrared (NIR) in some cases (Krbetschek et al., 1997). Filters are used in the instrumentation to restrict the emission to the UV so that the light from the stimulation is not collected by the photomultiplier tube measuring the emitted signal from the quartz. The De calculation is done using the single-aliquot regenerative-dose (SAR) protocol (Section 3.2.3) (Murray and Wintle, 2000, 2003).

OSL dating challenges in glacial systems and how to overcome them:

In OSL dating, it is assumed that the traps were nearly completely empty at the time of the burial of the grains. The depositional environment can play a crucial role in determining the degree of bleaching of the grains in a glacial environment.

The deposition of sediments in a glacial environment can result in two different types of bleaching: [1] homogeneously poorly bleached samples, where all the grains in the sample have been poorly bleached due to limited exposure to light (e.g., as in glacial lakes) and [2] heterogeneously bleached samples, which contain a mixture of well-bleached and poorly bleached grains, where some grains in the sample have been well-bleached, while others have

not been exposed to enough light to be fully bleached (e.g., in areas with a mixture of light exposure, such as glacial tills; Fuchs and Owen, 2008) (Figure 3.5).

In luminescence dating, partial bleaching of multi-grain aliquots is a critical issue. A multi-grain single aliquot is a sample composed of multiple grains from the same sediment, and it is used to determine the age of the sediment through Luminescence dating methods, such as OSL dating. Galbraith et al. (1999) highlight the importance of full bleaching of the grains in a multi-grain single aliquot sample. If the grains in the sample have not been fully bleached, the De (and OSL age) calculated from the sample will include residual dose from previous exposure to cosmic radiation and natural radioactivity in the soil, which can lead to an overestimation of the true age of the sediment when combined with the burial dose of interest. If the grains in the samples had not been completely bleached, then the De (and OSL age) measured from a multi-grain single aliquot will be too large as it will still have the residual dose along with the burial dose of interest (Galbraith et al., 1999). To counter this challenge, De measurements on single grains are done to isolate grains that have been fully bleached at the time of burial (Duller, 2008). Measurements made using single grain can capture the true variations in De, whereas, in the measurement of multi-grain, if we measure small aliquots of 50 or so grains, only a small proportion of those grains - and maybe even a single grain – dominates the signal. Thus, a small aliquot signal may tend towards a single grain signal.

Choosing between quartz and feldspar:

Past studies in glacial depositional environments have compared the bleaching of the luminescence signals in quartz and feldspar, concluding that the quartz signals are more easily bleached in full daylight than potassium feldspars and that inadequate bleaching of the infrared signal can give an overestimation of the feldspar ages (Spencer and Owen, 2004). However,

recent studies have investigated the relationship between mineral type, grain size, and the bleaching process and concluded that the degree of bleaching is dependent on both grain size and mineral type.

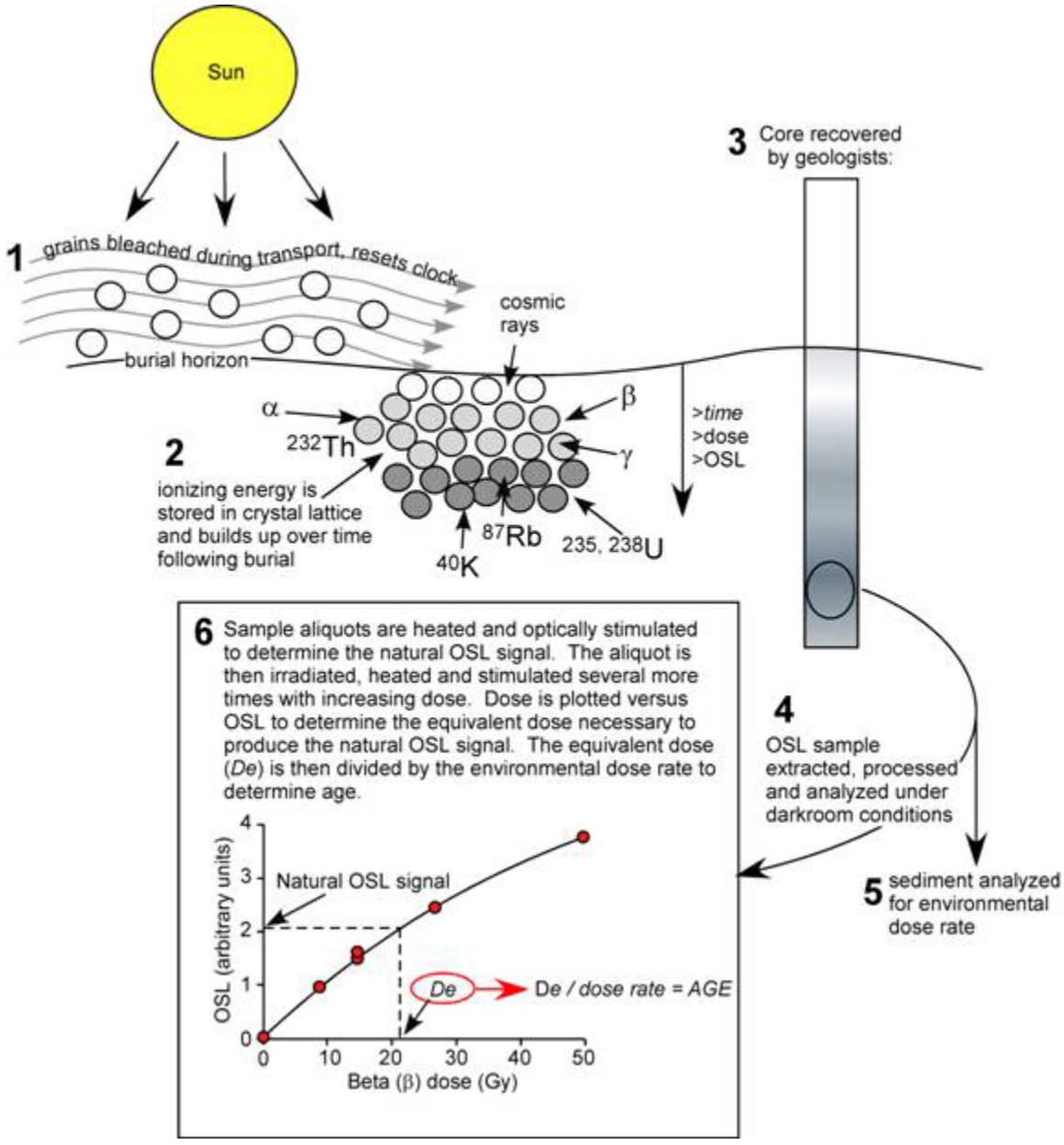

Figure 3.1: Schematic of generalized processes that produce the luminescence signal (steps 1 and 2), and the sampling and analytical procedure to determine age of deposition (steps 3 through 6) (after Mallinson, 2008).

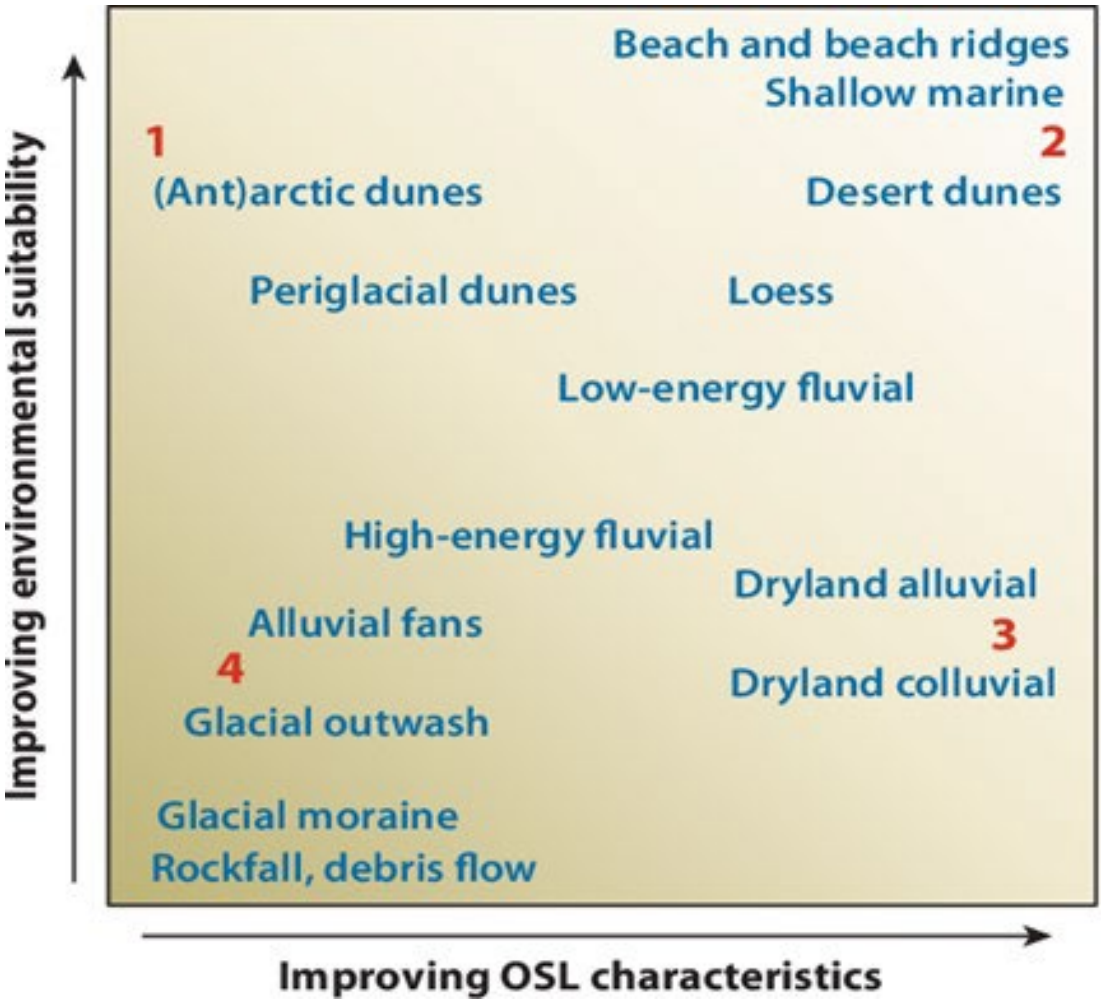

Figure 3.2: Degree of bleaching is a factor of environmental setting and sample characteristics. Quartz grains bleach differently based on light exposure and their environmental history; grains from well-lit areas like beaches bleach faster, while those recently eroded from bedrock bleach more slowly (Rhodes, 2011).

3.2.2 Sample collection and preparation

The sampling sites were chosen to determine the timing of the maximum extent of the Flathead Lobe. As explained in several past studies (Smith, 2004; Braden, 2006; Hofmann and Hendrix, 2010), the Polson Moraine has been identified as the terminal moraine for the Flathead Lobe. Two samples were taken from the Elmo Moraine, which has been identified as a lateral moraine of the terminal extent of the Flathead Lobe.

The surface of individual sampling sites was cleaned to remove any weathered and loose sediment and to expose primary bedding structures wherever possible ensuring that the samples being collected are representative of the original depositional environment and can provide more accurate OSL dates. Samples from glacial till were collected using steel tubes by hammering into the exposed surface. The tubes were covered with black tape and care was taken to minimize daylight exposure. A total of seven samples were collected of which five samples were from the Polson Moraine and two were from the Elmo Moraine (Section 2.1, Figure 2.1).

Preparation of samples from glacial moraines followed standard procedures as follows:

[1] Sediments at a depth of ~2 cm were removed from the end of each core to eliminate the possibility of analyzing grains that had undergone exposure to daylight during sample collection.

[2] Samples were prepared under very low-intensity amber LEDs. The combination of low- intensity and amber LED was used so that they do not erase any luminescence signal; this is specific for the preparation of feldspars minerals, but quartz minerals can also be prepared under these lamps.

All samples were weighed before drying them at 50°C in an oven after which they were weighed again. This step was done to assess field moisture in the samples as water attenuates the alpha, beta, and gamma radiation impact on the samples. [3] To separate grain-size fractions,

~100 g of the sediment from the middle of the core (unexposed to daylight) was dry sieved using mesh sizes of 90, 125, 170, 212, 250, and 300 μm. The selected grain size for each sample was the modal size for fractions <250 μm. This was the 125-170 μm fraction for five of the samples, namely Polson-03, Elmo-04 and -05, and Polson-06 and -07. For Polson-01 and -02, there was insufficient material in the 125-170 μm size fraction, and grains in the 90-125 μm

fraction were selected instead (Polson-01 didn't have enough sample left for analysis, thus it is not included in further measurements). [4] The selected grain size was treated with 10% hydrochloric acid (HCl) for ~30 min to remove any adhering carbonates, any reacted and suspended material decanted, and followed immediately by a 30% hydrogen peroxide (H2O2) wash for ~3 days to remove organic matter. After the H2O2 step, the samples were washed in deionized H2O (used to minimize any possibility of free ions in the water affecting the luminescence signals) to remove any remaining H2O2 and material in suspension, washed in acetone to drive off any remaining H2O, and dried in the oven for a few minutes until the grains were dry and flowed freely. [5] Quartz, plagioclase, and Na-rich feldspars (2.58 - 2.70 g/cm3) were separated from K-rich feldspars (< 2.58 g/cm3) using lithium metatungstate (LMT) solutions with densities of 2.70 g/cm3 and 2.58 g/cm3. [6] The quartz and feldspar fractions were washed in deionized H2O and acetone and briefly dried in the oven at 50°C. The quartz fractions were then treated with 48% HF for 40 min to dissolve plagioclase feldspar and Na-rich feldspars. The HF treatment also removes an ~10-20 μm rind from the quartz grains and in so doing minimizes the luminescence from alpha particles external to the grain. After this the samples were given a 10% HCl wash to dissolve any precipitated fluorides, and then deionized H2O, acetone, and drying steps repeated.

Multi-grain aliquots of quartz of 1-2 mm diameter were mounted in the center of ~10 mm stainless steel discs using silicone spray (Silkospray™) and spray templates. The number of grains on a 1-mm aliquot ranged from ~ 30-40 grains for 125-170 μm size and ~ 70-90 grains for 90-125 μm size.

3.2.3 OSL measurements and De assessment

All the multi-grain luminescence measurements were made at Kansas State University using a Risø TL/OSL reader model DA-20 (Bøtter-Jensen et al., 2003) equipped with a 90Sr/90Y beta source with a dose rate of ~ 0.118 Gy/s. Blue LEDs (470 nm) were used for quartz stimulation and signals were collected through 7.5 mm of Hoya U-340 (UV) filter.

The measurement sequence is outlined in Table 1.

The SAR protocol outlined in Table 1 is composed of six steps. Step 1 involves administering the regenerative dose, in run 1 for measurement of the natural dose, the regenerative dose is 0 Gy; step 2 involves pre-heating the sample for 10 s at a temperature of 240°C; this step enables us to remove unstable charge from shallower electron traps before we measure the stable dating signal. The preheat temperature is usually determined through a series of experiments in which the sample is heated to different temperatures, and the OSL signal is measured after each heating cycle. The temperature at which the OSL signal stabilizes is typically chosen as the preheat temperature. This process is repeated for multiple samples in order to establish a consistent preheat temperature for the dating analysis; step 3 involves measuring the luminescence signal (Lx); step 4 involves providing a fixed test dose (Dt) which is 15 - 25% of the average De; step 5 involves heating the sample to 200°C, the temperature varies with sample; step 6 involves measuring the test dose luminescence signal (Tx) relevant to the natural/administered OSL measurement. Measuring the test dose luminescence signal (Tx) allows for determination of the efficiency of the measurement system, which can vary from measurement to measurement. By comparing the natural or administered OSL signal of the sample to the test dose signal (Tx), the OSL dating system can be calibrated to accurately determine the dose of radiation that the sample has received and, subsequently, its age; step 7

involves administering the sample a hot bleach, the hot bleach step is particularly important for quartz, which can sometimes contain residual signals that are not fully removed by the preheat and blue light steps. By heating the sample to a high temperature, any remaining signals are bleached, allowing for a more accurate measurement of the OSL signal. Without the hot bleach step, the OSL signal from the sample may be artificially high, leading to inaccurate age estimates.

The above process used to calculate De values using the SAR procedure includes measuring the natural luminescence signal (Ln) occurring due to irradiation in nature, evaluating the sensitivity of the aliquot by measuring the luminescence signal (Tn), generated by a test dose (Dt), and then administering a number of cycles which involve irradiation (D1, D2, D3, etc.) to generate luminescence signal (L1, L2, L3, etc.) also note that one of the regenerative doses is recycled (same dose twice) and one is given a 0 dose (to determine if OSL is also 0 or has an elevated signal above 0), followed by a test of sensitivity (T1, T2, T3, etc.) using the test dose.

The value of De is calculated by comparing the ratio Rn (=Ln/Tn) with the ratios R1, R2, R3, etc. from the ratios of L1/T1, L2/T2, L3/T3 etc. that gives us a laboratory dose equivalent to the natural signal. A typical continuous wave (CW) OSL decay curve is shown in the Figure 3.6A; the corresponding SAR data and De value obtained is shown in Figure 3.6B. Using the SAR method, we tested the measurement of zero dose or the recuperation ratio test. Occasionally, due to charge recuperation, most usually subsequent to preheating treatments, a signal is observed even with zero dose applied. The recuperation test compares the Lx/Tx ratio for a zero regenerative dose to Ln/Tn. Data is accepted if this value is below 5%.

Table 1: SAR sequence based on Wintle and Murray, 2006. Equivalent doses (De) were calculated (steps 3 and 6).

Step	Treatment	Observed
1	Give regenerative dose	
2	Pre-heat: 240°C for 10 s (varies with sample)	
3	Blue LED stimulation: 40 s at 125°C	Lx (natural or regenerative dose OSL)
4	Test dose (Dt)	
5	Heat to 200°C (varies with sample)	
6	Blue LED stimulation: 40 s at 125°C	Tx (OSL response to a small test dose)
7	Heat to 280° C (varies with sample)	
8	Return to step 1 for run 2	

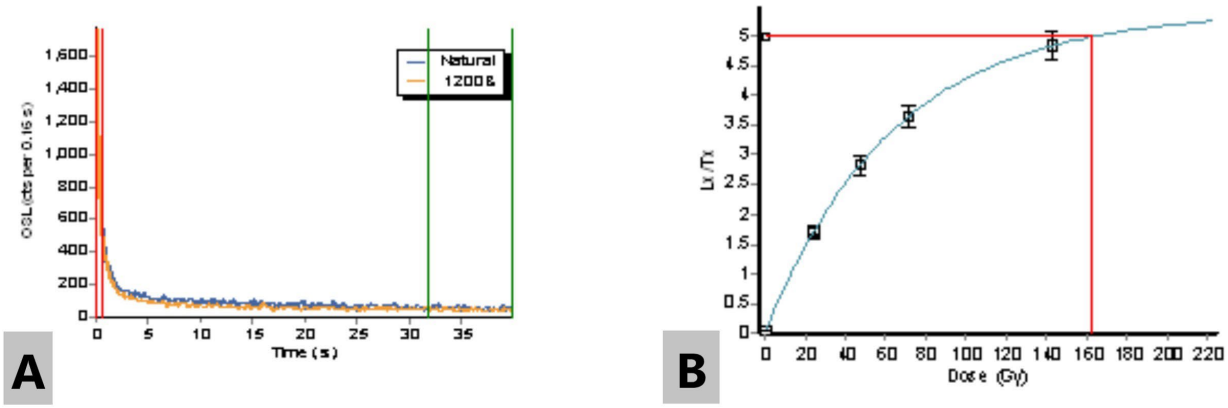

Figure 3 (A) CW OSL decay curve of quartz for sample Polson-06. The blue line shows the natural signal from the sample and the orange shows a regenerated 166.83 Gy dose. (B) Dose response curve for Polson-06, Recuperation ratio: 0.8 ± 0.3%. The sensitivity corrected natural OSL (Ln/Tn) is plotted on the Y axis (zero laboratory dose) and then interpolated to X axis with

the growth curve (blue line) fitted through successive regenerative dose points (Lx/Tx). Best fit growth curve is a single saturating exponential function. (De: 163.09 ± 41.66 Gy).

3.2.5 Recycling ratio test

The recycling ratio test is an essential step in OSL dating to verify the reliability of OSL measurements (Murray and Wintle, 2003). The test involves multiple irradiations of the sample with a known radiation dose, and the OSL signal is measured after each irradiation. Recycling ratio is the ratio of two Lx/Tx values for the same regenerative dose. It is usually the first and last regenerative dose points of the SAR cycle that are repeated in this way. A recycling ratio close to 1 indicates that there is no significant signal loss, and the OSL measurements are reliable. Once the recycling ratio test is successfully completed, routine measurements of the OSL signal resulting from a single radiation dose can be performed (Murray and Wintle, 2003) (Figure 3.6). The ratio between the two sensitivity-corrected luminescence signals is the recycling ratio, which should be ideally unity. However, a value within 10%, or between 0.9-1.1, is acceptable (Murray and Wintle, 2000; Wintle and Murray, 2006). For example, the recycling ratio for the sample Polson- 06 for i=1-6 in the figure above is 1.00 ± 0.07, which is within the acceptable limits.

3.2.6 Dose recovery tests

The dose recovery test is a widely used test with the SAR protocol in OSL dating. The test aims to determine if the SAR protocol can accurately measure a known dose of radiation and if it can measure the dose recovered from the sample (Murray and Wintle, 2003). Passing this test gives greater confidence in the SAR's ability to accurately measure the radiation dose and recoverable signal from the sample (Rhodes, 2011). For this task, the OSL signal from two aliquots from samples Polson-02, Polson-03, Elmo-04, Elmo-05, Polson-06, and Polson-07 was

zeroed, a 400 s regenerative dose administered, and the SAR carried out as indicated in Table 1. Table 2 shows the results of the dose recovery tests.

Table 2: Dose recovery test for the samples. Given dose is based on average De recorded for each sample. Results are the average measured/given (M/G) ratios for the samples.

Sample Name	Given	Measured	M/G
Polson – 02	350	462	1.32
Polson – 03	400	295	0.74
Elmo – 04	400	403.1	1.01
Elmo – 05	400	383.6	0.96
Polson – 06	400	386.4	0.97
Polson – 07	400	390.7	0.98

3.2.7 Environmental dose rate measurement

The environmental dose rate (usually expressed in Gy/ka or mGy/a) is required to determine an OSL age (Eqn. 1). The environmental dose rate is assessment of the exposure of mineral grains to ionizing radiation from the decay of the U and Th series, ^{40}K, ^{87}Rb, and cosmic sources during the burial period.

The dried exposed ends of the seven samples (~20 g) were pulverized into fine powder in a Shatterbox® using a tungsten carbide ring and puck mill. Approximately 10 g of powder from each sample was sent to SGS Canada Inc. in Ontario, Canada for ICP-AES/- MS analysis to determine the elemental concentrations of K, Th, U and Rb.

The environmental dose rate was calculated using the DRAC dose rate calculator (Durcan et al., 2015) (Table 3). For dose rate calculations, radionuclide conversion factors from Guérin et al. (2011) were used. The grain size attenuation factor for the beta dose rate was selected after

Guérin et al. (2012). The calculation of the cosmic dose rate was based on Prescott and Hutton (1994). Water content of the sample was determined when the samples were brought to the lab by comparing weight of sample plus moisture with the dried sample after weight stabilization in the oven at 50°C.

Table 3: Sample radioactive nuclide concentrations, and dose rate analysis of samples.

Sample Name	Longitude & Latitude	Elevation (m)	Grain Size (µm)	Cosmic dose rate (Gy/ka)	Depth of Overburden (m)	Water Content (%)	U (ppm)	Th (ppm)	K (%)	Rb (ppm)	Dose rate (Gy/ka)
Polson-01	47^{0}41'22.20" N 114^{0}14'13.72" W	999	90-125	0.19 ± 0.02	~ 2	0.041	2.74	9.7	2.6	111	3.94 ± 0.17
Polson-02	47^{0}40'43.04" N 114^{0}16'58.74" W	946	90-125	0.14 ± 0.01	~ 4.5	0.040	3.01	11	2.6	111	4.04 ± 0.17
Polson-03	47^{0}38'27.72" N 114^{0}7'42.46" W	972	125-170	0.23 ± 0.02	~ 1	0.047	1.46	5.2	1.8	57.9	2.60 ± 0.16
Elmo-04	47^{0}49'14.29" N 114^{0}23'30.03" W	1030	125-170	0.19 ± 0.02	~ 2	0.039	1.68	6.6	2	77.7	2.89 ± 0.16
Elmo-05	47^{0}49'12.84" N 114^{0}23'31.89" W	1033	125-170	0.22 ± 0.02	~ 2	0.017	1.88	7	1.8	64.5	2.80 ± 0.16
Polson-06	47^{0}39'48.72" N 114^{0}8'35.42" W	977	125-170	0.18 ± 0.02	~ 3	0.010	1.23	4.5	1.4	42.8	3.07 ± 0.17
Polson-07	47^{0}39'46.81" N 114^{0}8'42.09" W	969	125-170	0.13 ± 0.01	~ 2	0.169	2.07	6.8	2.1	70.1	3.02 ± 0.17

3.2.8 Equivalent dose data

Equivalent dose distribution and ages were calculated using the central age model (CAM) (Galbraith et al., 1999). The equivalent dose data in Figure 3.7 is represented using the Abanico plot, based on the combination of a radial plot and a kernel density estimate curve (Galbraith and

Green, 1990). The abanico plot as created by the default R function call (plot_AbanicoPlot(…)) using the example data provided with the R package "Luminescence".

3.2.8.1 – Multi grain aliquots

De results are calculated based on multi-grain (90-125 μm and 125-170 μm) quartz measurements, performed on a Risoe TL/OSL DA-20 reader. Abanico plots were created to show the De distribution for the samples. The plot consists of two parts, a bivariate plot (a radial plot) on the left side and a univariate plot (by default a kernel density estimate, KDE) on the right side. De values are shown on a log-scale.

The dark gray shaded area in the middle of the plot represents dispersion bar for the dataset, the dashed line in the middle is the central value line, the lines on the outside of the plot represent the plot frame, the light gray shaded area in the middle is the scatter polygon, the dots represent the data points and the lines on the inside of the plot represent grid line/isochron. The curved line on the right side of the graph represents the KDE curve. The example shows the different components of the graph (Figure 3.7).

The abanico plots for four samples (Elmo-04, Elmo-05, Polson-06, and Polson- 07) were chosen as examples to show the distributions of equivalent dose (De) using the luminescence R language (Dietze et al., 2016) (Figure 3.8-3.11). Polson -01 did not have enough material left thus no further analysis was made on the sample. Polson -03 had only three data points that passed the overall criteria for measurement thus did not include its abanico plots. The De frequency distributions based on the SAR protocol are shown as a radial plot of De on the left side, while a kernel density estimate curve of De is shown on the right side. Using Polson-06 as an example, the median value of De is 2100s (247.8 Gy) with 41.7% of De values within 2σ. The

kernel density estimates curve, and the histogram are effective at visualizing the De distribution. The radial graphs allow visualization of over-dispersion, represented by those points beyond two standard errors.

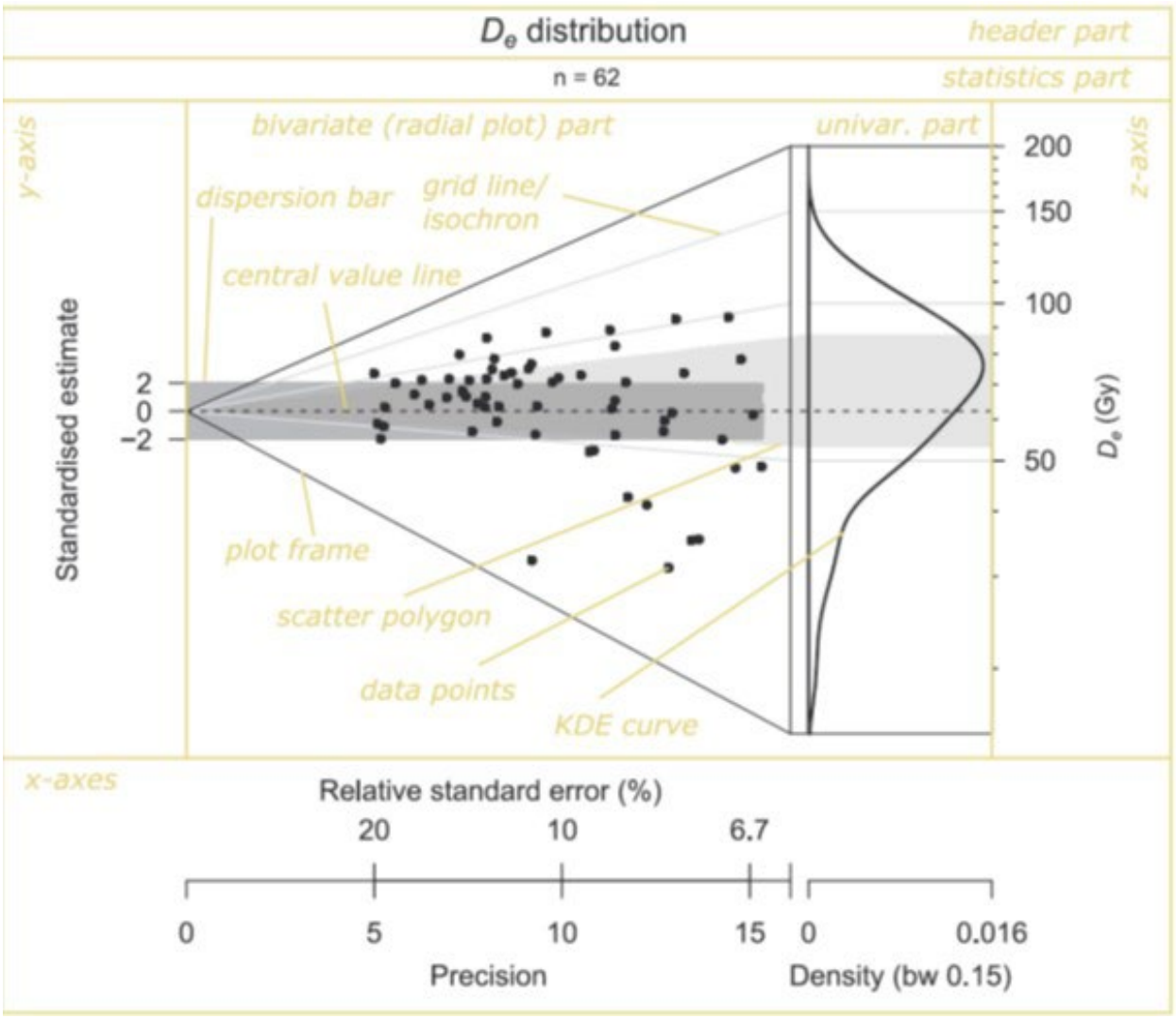

Figure 4: The abanico plot as created by the default R function call (plot_AbanicoPlot(...)) using the example data provided with the R package 'Luminescence' (ExampleData.DeValues $CA1), results based on single grain (200–250 \si\micron) quartz measurements, performed on a Risoe TL/OSL DA-20 reader at the University of Cologne). The plot consists of two parts, a bivariate plot (a radial plot) on the left side and a univariate plot (by default a kernel density estimate) on the right side. De values are shown on a log-scale (after Dietze et al., 2016).

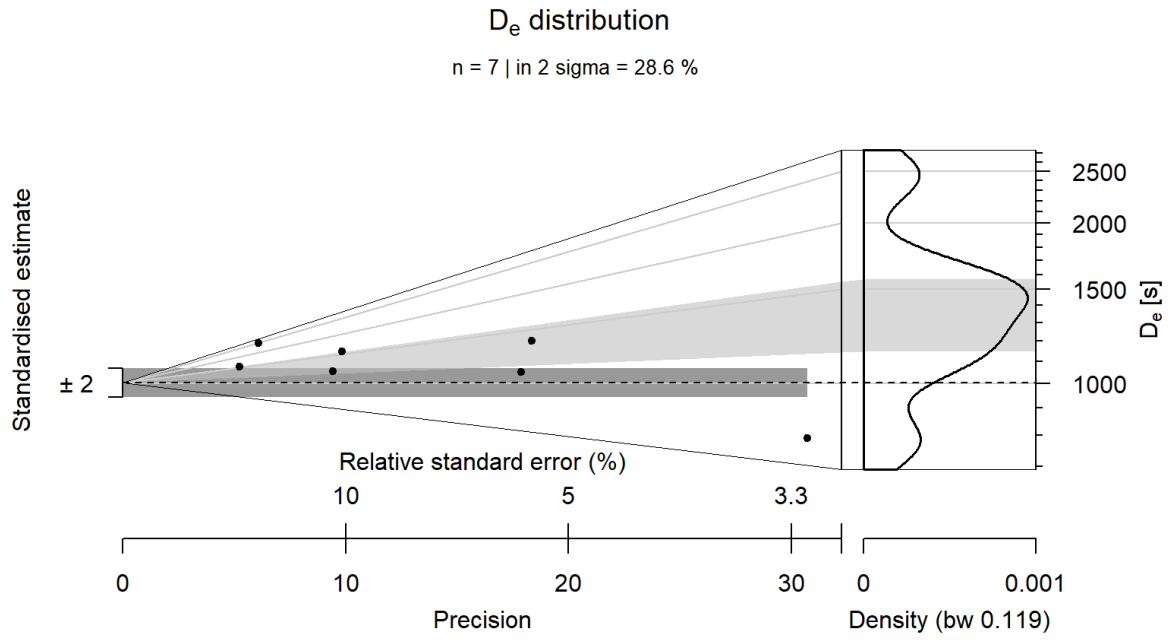

Figure 5: The abanico plot of Elmo-04. The abanico plot consists of two parts: a bivariate part (showing standardized estimates in relation to the precisions) and a univariate part (showing the age frequency distribution) (Dietze et al., 2016). The plots include a radial plot of De on the left side, a kernel density estimate curve, and a histogram of De on the right side for each sample.

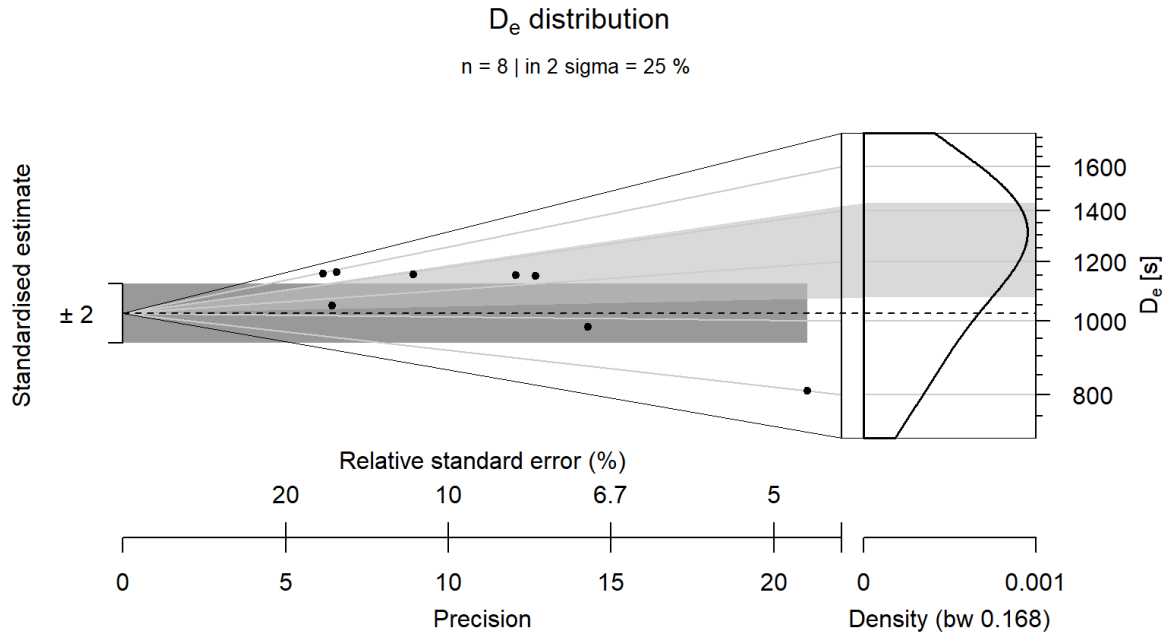

Figure 6: The abanico plot of Elmo-05. The abanico plot consists of two parts: a bivariate part (showing standardized estimates in relation to the precisions) and a univariate part (showing the

age frequency distribution) (Dietze et al., 2016). The plots include a radial plot of De on the left side, a kernel density estimate curve, and a histogram of De on the right side for each sample.

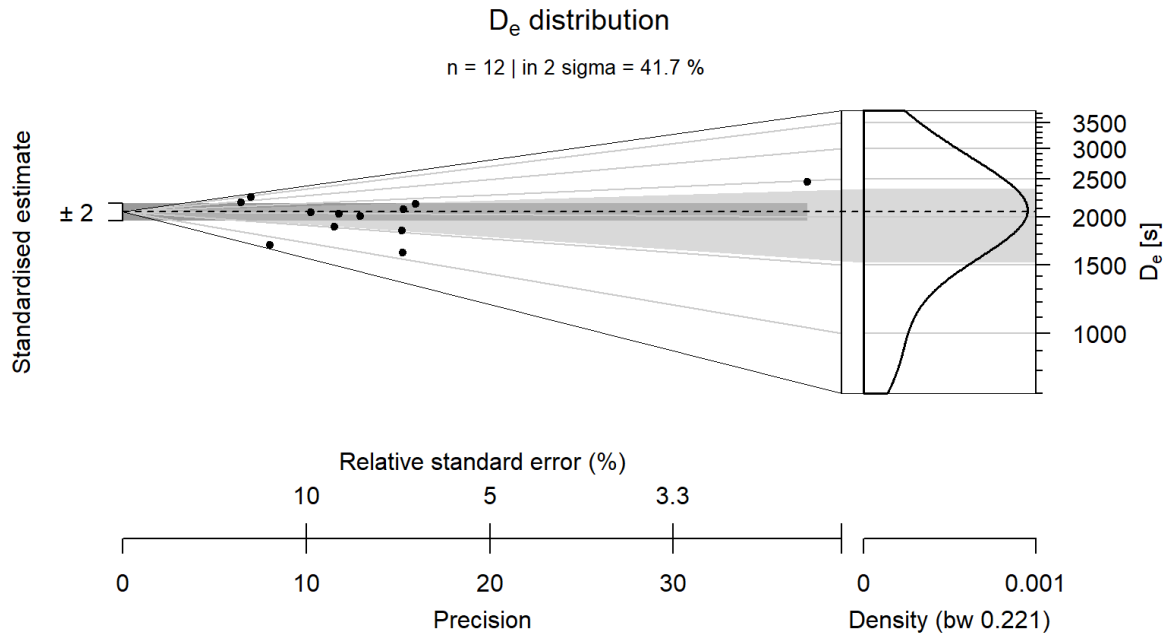

Figure 7: The abanico plot of Polson-06. The abanico plot consists of two parts: a bivariate part (showing standardized estimates in relation to the precisions) and a univariate part (showing the age frequency distribution) (Dietze et al., 2016). The plots include a radial plot of De on the left side, a kernel density estimate curve, and a histogram of De on the right side for each sample.

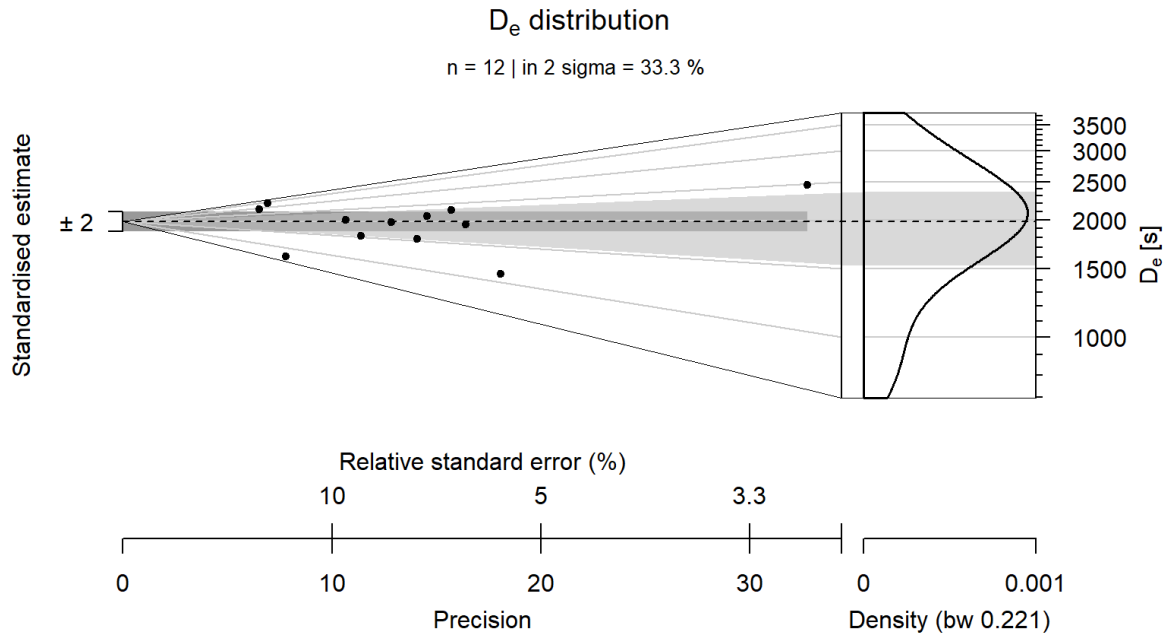

Figure 8: The abanico plot of Polson-07. The abanico plot consists of two parts: a bivariate part (showing standardized estimates in relation to the precisions) and a univariate part (showing the age frequency distribution) (Dietze et al., 2016). The plots include a radial plot of De on the left side, a kernel density estimate curve, and a histogram of De on the right side for each sample.

3.2.9 OSL age calculation

The commonly used statistical methods for calculating De values range from the simple use of the mean or weighted mean to models with internal assumptions of De distributions, sediment bleaching, and scatter. The central age model (CAM, Galbraith et al., 1999) is best applied in settings where all the grains were fully zeroed (bleached) at the time of the event. The Common Age model of Galbraith et al (1999) works with the natural log of the De values, any zero or negative De values are ignored. In this study, overdispersion was evaluated using a methodology proposed by Galbraith et al. (1999), which involves an iterative approach to quantify the degree of scatter in the data beyond what can be attributed to experimental uncertainties such as counting statistics and instrumental errors. Specifically, this method was applied to a set of equivalent dose values and their respective uncertainties. Note: For the sample

Polson-03, multiple replicates were done but only three passed the overall criteria for OSL measurement.

Table 4: Equivalent dose (De) modeling results. For each sample the De is modeled based on the central age model (CAM) and Common Age model with the luminescence software package in R program. n indicates the number of aliquots used for each sample. OD is the overdispersion in the CAM model.

Sample	n	De (Gy) CAM	De (Gy) Common Age	Overdispersion (%)
Polson - 02	12	160.2 ± 5.5	163.1 ± 14.3	24.1 ± 2.3
Polson – 03	3	39 ± 2.3	78.5 ± 45.6	51.7 ± 9.3
Elmo – 04	13	145.1 ± 3.8	184.4 ± 23.9	44 ± 2.7
Elmo – 05	13	127.1 ± 3.2	140.4 ± 10	22.1 ± 1.6
Polson – 06	12	160.2 ± 5.5	163.1 ± 14.3	24.1 ± 2.3
Polson – 07	15	101.3 ± 3.2	122.8 ± 32.4	41.7 ± 14.8

Table 5: Calculated ages based on the preferred De values.

Sample	Dose rate (Gy/ka)	De (Gy) CAM	Age (ka)
Polson – 02	4.04 ± 0.17	160.2 ± 5.5	39.7 ± 1.9
Polson – 03	2.60 ± 0.16	39 ± 2.3	15 ± 1
Elmo – 04	2.89 ± 0.17	145.1 ± 3.8	50.1 ± 1.5
Elmo – 05	2.80 ± 0.16	127.1 ± 3.2	45.4 ± 1.5
Polson – 06	3.08 ± 0.17	160.2 ± 5.5	52.1 ± 2.9
Polson - 07	3.02 ± 0.17	101.3 ± 3.2	33.5 ± 1.9

Chapter 4 - Discussion

The study aimed to refine the glacial chronology of the southeastern extent of the Cordilleran Ice Sheet (CIS) using the OSL dating technique to constrain the age of the glacial features associated with the terminal moraine (Polson) of the Flathead Lobe.

The Flathead Valley and all its neighboring mountainous area were covered by glacial ice during latest Pleistocene time, though there may have been nunataks or exposed peaks that were not completely covered by ice (~15,000-25,000 yr). Tracing glacial sequences has been challenging due to the erosion and subsequent sediment burial that transpired during the latest glacial period. The (CIS) had spread into the Puget Lowland and Juan de Fuca Strait by approximately 21 ka, while it had merged with a separate glacier in Barclay Sound to the west of Vancouver Island after overtopping the island. By 17.5 ka, the CIS had reached its maximum extent in Washington, with the Juan de Fuca Lobe stretching westward to the continental shelf, and several large lobes such as the Puget, Okanogan, Columbia River, Purcell Trench, and Flathead lobes extending southwards (Hendy, 2009).

The ages obtained from the OSL dating technique in this study are most significantly greater than the expected value of ~17.5 ka, which is the last glacial maximum age of Juan de Fuca lobe of the western CIS (Hendy, 2009).

The ages obtained from the Polson Moraine range from 14.98 ± 0.97 ka (Polson-03) to 52.08 ± 2.86 ka (Polson-06), while the ages obtained from the Elmo Moraine range from 45.36 ± 1.50 ka (Elmo-05) to 50.1 ± 1.5 ka (Elmo-04) (Table 5) except for Polson-01 for which there was not enough sample material left for analysis. These ages are representative of different geological events that occurred during the last glacial maximum of the cordilleran ice sheet in northwestern

Montana. The Polson-02 sample was collected from the northern Polson Moraine. It sits next to the Flathead River and is composed of hoodoo-like sandy silt deposits. The age of Polson-02 is ~39 ka years suggesting that these sediments were deposited during the end of the Pleistocene glaciation period, carried by meltwater streams and rivers, eventually deposited downstream. Polson-03 sample was collected immediately south of southern Polson moraine and is mapped as a Quaternary alluvium (Qal) deposit in the geological map (Vuke et al., 2007). The age of Polson-03 is ~15 ka is the closest to the ages of the last glacial maximum in the western CIS somewhere near 17.5 ka and the ages of 18.6 to 24.3 ka obtained from delta foresets in Dayton Creek Delta (Spencer & Spencer, 2019). The ~15 ka age of Polson- 03 suggests that sediment-laden meltwater from the Flathead Lobe flowed down the from the southern Polson moraine and resulted in the deposition of stratified deposits of sorted alluvium sediments. Polson-06 and Polson-07 samples were collected from the southern part of the Polson Moraine. Polson-06 is dated to be ~52 ka years and was collected from sandy laminated beds at the top of the outcrop. The sandy laminated beds suggest a steady sediment deposition, likely in a glacial lake environment, resulting from the combined effect of glacial activity and meltwater streams. Polson-07 is dated to be ~33 ka years and was collected from the basal laminated beds at the bottom of the outcrop. The basal laminated beds suggest another period of steady sediment deposition, forming the stratified layers from which the sample was taken. The difference in these dates, along with the differences in sedimentological character, suggests two major periods of deposition in the southern arm of the Polson Moraine, which is believed to have formed under subaqueous conditions (Hofmann et al., 2006). The age reversal between Polson-06 and Polson-07 might be because Polson-06 may have undergone significantly more acute partial bleaching than Polson-07 which may be related to differing mechanisms of deposition for sediments at the

top of the outcrop compared to basal sediments. Elmo-04 and Elmo-05 were collected from a site composed mainly of Quaternary glacial till and a mixture of poorly sorted sands and gravel (Vuke et al., 2007). The age of Elmo-04 is ~50 ka years and Elmo-05 is ~ 45 ka years; the sediment package was likely formed due to glacial activity and subsequent lacustrine or slow-moving water body deposition.

These ages suggest that the Flathead Lobe may have experienced multiple phases of advance and retreat, rather than a single glacial maximum. The obtained ages are most likely overestimated due to the challenges with OSL dating of glacial sediments such as partial bleaching or limited/absent exposure of the sediments to sunlight, which is necessary for resetting the OSL signal, incomplete resetting of the OSL signal due to previous exposure to sunlight or another source of ionizing radiation or mixing of different OSL signals due to mixing of sediment from different sources, such as sediment deposited during multiple glaciations. Considering the limited number of repeat SAR runs (with the maximum being only 15) and the evident scatter in the Abanico plots, it's challenging to draw a definitive interpretation of the ages obtained. The ages identified in the samples are likely to be apparent ages rather than the true ages of burial. Such apparent ages are significantly influenced by partial bleaching. Unlike a scenario where true ages might be influenced by the mixing of older sediments, the evidence in this study strongly points to partial bleaching as the primary factor.

However, the ages also suggest that the glacial history of the area is more complex than previously thought. The study collected samples from different depositional environments, including Quaternary till deposit (Qgt), Quaternary glacial lake deposits (Qgl), and Quaternary alluvium (Qal) deposits, providing a comprehensive understanding of the glacial history of the study area and the sedimentary processes that took place. The Polson Moraine samples as noted

by Bondurant (2005), for example, exhibit climbing current ripples, suggesting a subaqueous depositional environment, while the Elmo Moraine has poorly sorted sands and gravel with fluvial channels extending from it, indicative of supraglacial flow.

The sample descriptions, which highlight the depositional environment, the characteristics of the sediments, and the overburden of each sampling site (which can affect the dose rate calculation, that is used to determine the total amount of radiation that the sediment has received since the last exposure to sunlight).

The overestimate of age by OSL dating technique may be due to the challenge of ice-proximal settings. The overestimation can be attributed to incomplete bleaching of the sediments, due to presence of basal sediments, turbidity in water, proximity of the sediments to glacier or short distance travelled. Due to these reasons sediments may receive insufficient exposure to sunlight or a lack of transport of the sediment to the surface. This may result in an overestimate of the depositional age. To minimize this effect, the study employed small aliquot OSL analysis method. However, even these methods could not eliminate the potential for overestimation.

Possible future work may include a facies approach to OSL sampling of glacial sediments to obtain sediments that have been sufficiently bleached to reset the luminescence signal before deposition. Re-examination of the samples using other dating techniques to cross-check and verify the obtained ages. With the existing samples, single grain analysis dating approach could be explored, feldspar grains could be dated to compare them with the quartz obtained ages and more replicates of quartz could be explored. The study area could also be expanded to cover a larger region to provide a more comprehensive understanding of the glacial history of the area thus enabling to collect well bleached samples for OSL dating. Further studies could focus on

specific depositional environments to provide a more detailed understanding of the sedimentary processes that occurred during the glacial period.

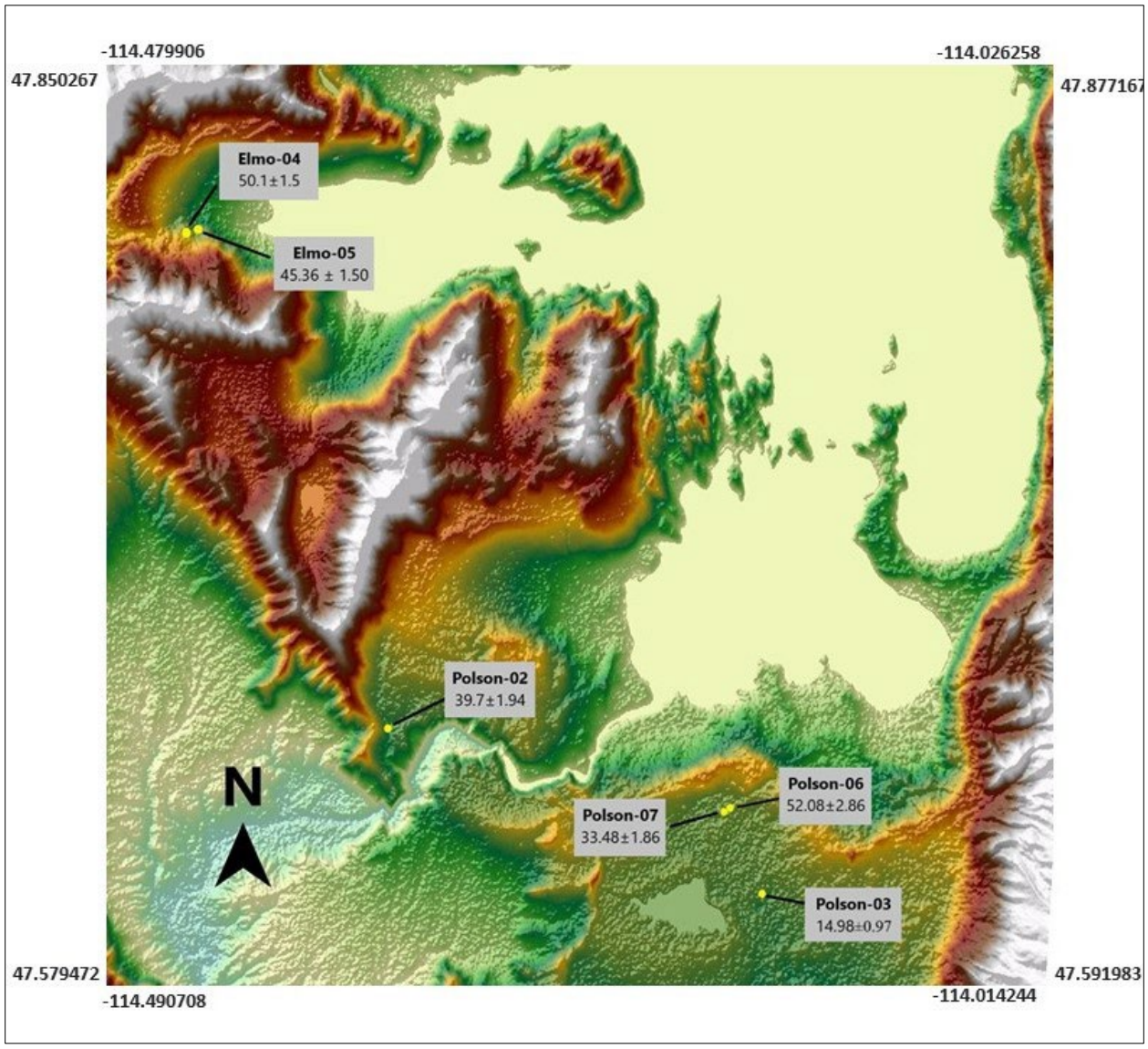

Figure **9**: Topographic map displaying the OSL ages obtained during this study at each sampling sites.

Chapter 5 - Summary and Conclusion

The study explored the late Pleistocene glacial history of the Flathead Lobe of the CIS and compared it with the western CIS chronology. Seven samples were collected from various depositional environments and dated via OSL geochronology, to provide a comprehensive understanding of the glacial history and sedimentary processes that took place in this region. Add a sentence here with the ages obtained, or at the very least, the age range you obtained. Limitations to small-aliquot OSL dating of quartz sediments from the Polson and Elmo Moraine were encountered. These limitations were reflected in age overestimates, which can be attributed to incomplete bleaching and lack of insufficient exposure to sunlight of the quartz grains. Geochronological and glacial geomorphological study of the region provide valuable insights into the depositional environment and the past glacial history of the area such as the subaqueous deposition of sediments, proximity of the sediments to glacier, and distance travelled by sediments before being deposited.

This research contributes to an expanding collection of current and previous research that may eventually be connected to examine the hypothesis that Pleistocene glacial advances are synchronous between the western CIS and eastern CIS. This research uses a combination of OSL geochronology, glacial geomorphology, and geospatial studies to determine the Polson Moraine of the Flathead Lobe as the maximum extent of the CIS in NW Montana.

Preliminary results from the Flathead Lobe suggest that bleaching potential of these glacial sediments is influenced by facies and depositional environment. The results advocate for a facies approach to OSL sampling of glacial sediments to obtain sediments that have been sufficiently bleached to reset the luminescence signal before deposition.

Possible future work includes the re-examination of the samples using other dating techniques to cross-check and verify the obtained ages. The study area could also be expanded to cover a larger region to provide a more comprehensive understanding of the glacial history of the area. Additionally, further studies could focus on specific depositional environments to provide a more detailed understanding of the sedimentary processes that occurred during the glacial period.

References

Alden, W.C., 1932, Physiography and Glacial Geology of Eastern Montana and Adjacent Areas: U.S. Government Printing Office, 214 p.

Batchelor, C.L., Margold, M., Krapp, M., Murton, D.K., Dalton, A.S., Gibbard, P.L., Stokes, C.R., Murton, J.B., and Manica, A., 2019, The configuration of Northern Hemisphere ice sheets through the Quaternary: Nature Communications, v. 10, p. 3713, doi:10.1038/s41467-019-11601-2.

Bondurant, A., 2005, Geologic mapping and sedimentologic analysis of Quaternary deposits along the western shore of Flathead Lake northwest Montana; documenting the record of deglaciation: Graduate Student Theses, Dissertations, & Professional Papers, https://scholarworks.umt.edu/etd/8981.

Bøtter-Jensen, L. & Mckeever, Stephen & Wintle, A.G. (2003). Chapter 1. Introduction. 10.1016/B978-044450684-9/50088-X.

Braden, Jason R., "History of syn-glacial and post-glacial sedimentation at the former terminus of the Flathead ice lobe near Polson Montana" (2006). Graduate Student Theses, Dissertations, & Professional Papers. 4684. https://scholarworks.umt.edu/etd/4684

Carrara, P.E., Short, S.K., and Wilcox, R.E., 1986, Deglaciation of the Mountainous Region of Northwestern Montana, U.S.A., as Indicated by Late Pleistocene Ashes: Arctic and Alpine Research, v. 18, p. 317–325, doi:10.1080/00040851.1986.12004093.

Clark, P.U., Dyke, A.S., Shakun, J.D., Carlson, A.E., Clark, J., Wohlfarth, B., Mitrovica, J.X., Hostetler, S.W., and McCabe, A.M., 2009, The Last Glacial Maximum: Science, v. 325, p. 710–714, doi:10.1126/science.1172873.

Cuffey, K.M., and Marshall, S.J., 2000, Substantial contribution to sea-level rise during the last interglacial from the Greenland ice sheet: Nature, v. 404, p. 591–594, doi:10.1038/35007053.

Dalton, A.S. et al., 2020, An updated radiocarbon-based ice margin chronology for the last deglaciation of the North American Ice Sheet Complex: Quaternary Science Reviews, v. 234, p. 106223, doi: 10.1016/j.quascirev.2020.106223.

Davis, W.M., 1920, FEATURES OF GLACIAL ORIGIN IN MONTANA AND IDAHO: A Shaler Memorial Study: Annals of the Association of American Geographers, v. 10, p. 75–147, doi:10.1080/00045602009357015.

Dickinson, W.R., 2004, Evolution of the North American Cordillera: Annual Review of Earth and Planetary Sciences, v. 32, p. 13–45, doi: 10.1146/annurev.earthdoi: 10.1146/annurev.earth.32.101802.120257.

Dietze M, Kreutzer S, Burow C, Fuchs MC, Fischer M, Schmidt C (2016). "The abanico plot: visualising chronometric data with individual standard errors." Quaternary Geochronology, 31, 12-18. doi: 10.1016/j.quageo.2015.09.003.

Duller, G. a. T., 2008, Single-grain optical dating of Quaternary sediments: why aliquot size matters in luminescence dating: Boreas, v. 37, p. 589–612, doi:10.1111/j.1502-3885.2008.00051. x.

Duller, G.A.T., 2012, Improving the accuracy and precision of equivalent doses determined using the optically stimulated luminescence signal from single grains of quartz: Radiation Measurements, v. 47, p. 770–777, doi: 10.1016/j.radmeasdoi: 10.1016/j.radmeas.2012.01.006.

Durcan, J.A., King, G.E., and Duller, G.A.T., 2015, DRAC: Dose Rate and Age Calculator for trapped charge dating: Quaternary Geochronology, v. 28, p. 54–61, doi: 10.1016/j.quageodoi: 10.1016/j.quageo.2015.03.012.

Dyke, A.S., 2004, An outline of North American deglaciation with emphasis on central and northern Canada, in Ehlers, J. and Gibbard, P.L. eds., Developments in Quaternary Sciences, Elsevier, Quaternary Glaciations-Extent and Chronology, v. 2, p. 373–424, doi:10.1016/S1571-0866(04)80209-4.

Dyke, A.S., Andrews, J.T., Clark, P.U., England, J.H., Miller, G.H., Shaw, J., and Veillette, J.J., 2002, The Laurentide and Innuitian ice sheets during the Last Glacial Maximum: Quaternary Science Reviews, v. 21, p. 9–31, doi:10.1016/S0277-3791(01)00095-6.

Edwards, J., 2006, Evidence for Glacial Outburst Floods along the Lower Flathead River: Results from Geologic Mapping, Geomorphologic Analysis and a Gravity Survey near Polson, Montana: Graduate Student Theses, Dissertations, & Professional Papers, https://scholarworks.umt.edu/etd/1211.

Fraser, K.I., Enkelmann, E., Jess, S., Gilbert, H., and Grieco, R., 2021, Resolving the Cenozoic History of Rock Exhumation Along the Central Rocky Mountain Trench Using Apatite Low-Temperature Thermochronology: Tectonics, v. 40, p. e2021TC006847, doi:10.1029/2021TC006847.

Fuchs, M., and Owen, L., 2008, Luminescence dating of glacial and associated sediments: Boreas, v. 37, p. 636–659, doi:10.1111/j.1502-3885.2008.00052. x.

Galbraith, R.F., Roberts, R.G., Laslett, G.M., Yoshida, H., and Olley, J.M., 1999, optical dating of single and multiple grains of quartz from jinmium rock shelter, northern australia: part i, experimental design and statistical models: archaeometry, v. 41, p. 339–364, doi:10.1111/j.1475-4754. 1999.tb00987. x.

Guérin, Guillaume & Mercier, Norbert & Adamiec, Grzegorz. (2011). Dose-rate conversion factors: Update. Ancient TL. 29. 5-8.

Guérin, G., Mercier, N., Nathan, R., Adamiec, G., and Lefrais, Y., 2012, On the use of the infinite matrix assumption and associated concepts: A critical review: Radiation Measurements, v. 47, p. 778.

Hanson, M.A., Lian, O.B., and Clague, J.J., 2012, The sequence and timing of large late Pleistocene floods from glacial Lake Missoula: Quaternary Science Reviews, v. 31, p. 67–81, doi: 10.1016/j.quascirevdoi: 10.1016/j.quascirev.2011.11.009.

Heller, P.L., Bowdler, S.S., Chambers, H.P., Coogan, J.C., Hagen, E.S., Shuster, M.W., Winslow, N.S., and Lawton, T.F., 1986, Time of initial thrusting in the Sevier orogenic belt, Idaho-Wyoming and Utah: Geology, v. 14, p. 388–391, doi:10.1130/0091-7613(1986)14<388: TOITIT>2.0.CO;2.

Hendy, I., 2009, A fresh perspective on the Cordilleran Ice Sheet: Geology, v. 37, p. 95–96, doi:10.1130/focus012009.1.

Hofmann, M.H., and Hendrix, M.S., 2010, Depositional processes and the inferred history of ice-margin retreat associated with the deglaciation of the Cordilleran Ice Sheet: The sedimentary record from Flathead Lake, northwest Montana, USA: Sedimentary Geology, v. 223, p. 61–74, doi: 10.1016/j.sedgeodoi: 10.1016/j.sedgeo.2009.10.004.

Hofmann, M.H., Hendrix, M.S., Moore, J.N., and Sperazza, M., 2006, Late Pleistocene and Holocene depositional history of sediments in Flathead Lake, Montana: Evidence from high-resolution seismic reflection interpretation: Sedimentary Geology, v. 184, p. 111–131, doi: 10.1016/j.sedgeodoi: 10.1016/j.sedgeo.2005.09.019.

Johnson, A.N., Sievert, R., Durglo, M., Finley, V., Adams, L., and Hofmann, M.H., 2014, Indigenous Knowledge and Geoscience on the Flathead Indian Reservation, Northwest Montana: Implications for Place-Based and Culturally Congruent Education: Journal of Geoscience Education, v. 62, p. 187–202, doi:10.5408/12-393.1.

King, G.E., Robinson, R.A.J., and Finch, A.A., 2014, Towards successful OSL sampling strategies in glacial environments: deciphering the influence of depositional processes on bleaching of modern glacial sediments from Jostedalen, Southern Norway: Quaternary Science Reviews, v. 89, p. 94–107, doi: 10.1016/j.quascirevdoi:10.1016/j.quascirev.2014.02.001.

Krbetschek, M.R., Götze, J., Dietrich, A., and Trautmann, T., 1997, Spectral information from minerals relevant for luminescence dating: Radiation Measurements, v. 27, p. 695–748, doi:10.1016/S1350-4487(97)00223-0.

LaPoint, D., 1971, Geology and geophysics of the southwestern Flathead Lake region Montana: Graduate Student Theses, Dissertations, & Professional Papers, https://scholarworks.umt.edu/etd/7182.

Levish, D.R. Late Pleistocene sedimentation in glacial Lake Missoula and revised glacial history of the Flathead lobe of the Cordilleran ice sheet, Mission Valley, Montana [Ph.D.]: University of Colorado at Boulder, 191 p.,

https://www.proquest.com/docview/304341346/abstract/81411CB549B24E0DPQ/1 (accessed April 2023).

Lisiecki, L.E., and Raymo, M.E., 2007, Plio–Pleistocene climate evolution: trends and transitions in glacial cycle dynamics: Quaternary Science Reviews, v. 26, p. 56–69, doi: 10.1016/j.quascirevdoi: 10.1016/j.quascirev.2006.09.005.

Locke, W.W., 1995, Modelling of icecap glaciation of the northern Rocky Mountains of Montana: Geomorphology, v. 14, p. 123–130, doi:10.1016/0169-555X (95)00053-5.

Lønne, I., 1995, Sedimentary facies and depositional architecture of ice-contact glaciomarine systems: Sedimentary Geology, v. 98, p. 13–43, doi:10.1016/0037-0738(95)00025-4.

Lukas, S., Spencer, J., Robinson, R., and Benn, D., 2007, Problems associated with luminescence dating of Late Quaternary glacial sediments in the NW Scottish Highlands: Quaternary Geochronology, v. 2, p. 243–248, doi: 10.1016/j.quageodoi: 10.1016/j.quageo.2006.04.007.

Mallinson, D., Burdette, K., Mahan, S., Brook, G., 2008. Optically stimulated luminenscence age controls on late Pleistocene and Holocene coastal lithosomes, North Carolina, USA. Quaternary Research 69, 97-109.

Mauk, J.L., 1983. Stratigraphy and sedimentology of the Proterozoic Burke and Revett Formations, Belt Supergroup, western Montana. Abstracts with Programs-Geological Society of America. Boulder, CO, USA, p. 424.

MBMG-Montana Bureau of Mines & Geology, http://www.mbmg.mtech.edu/mbmgcat/public/ListCitation.asp?pub_id=30078&#gsc.ta=0 (accessed April 2023).

Mudge, M. R., 1967: Surficial geologic map of the Sawtooth Ridge quadrangle, Teton and Lewis and Clark Counties, Montana. Scale 1:24,00. U.S. Geological Survey Geologic Quadrangle Map, GQ-991.

Murray, A.S., and Wintle, A.G., 2000, Luminescence dating of quartz using an improved single-aliquot regenerative-dose protocol: Radiation Measurements, v. 32, p. 57–73, doi:10.1016/S1350-4487(99)00253-X.

Murray, A.S., and Wintle, A.G., 2003, The single aliquot regenerative dose protocol: potential for improvements in reliability: Radiation Measurements, v. 37, p. 377–381, doi:10.1016/S1350-4487(03)00053-2.

Rhodes, E.J., 2011, Optically Stimulated Luminescence Dating of Sediments over the Past 200,000 Years: Annual Review of Earth and Planetary Sciences, v. 39, p. 461–488, doi:10.1146/annurev-earth-040610-133425.

Rittenour, T.M., 2008, Luminescence dating of fluvial deposits: applications to geomorphic, palaeoseismic and archaeological research: Boreas, v. 37, p. 613–635, doi:10.1111/j.1502-3885.2008.00056. x.

Saleeby, J.B., Busby-Spera, C., Oldow, J.S., Dunne, G.C., Wright, J.E., Cowan, D.S., Walker, N.W., and Allmendinger, R.W., 1992, Early Mesozoic tectonic evolution of the western

U.S. Cordillera*, in Burchfiel, B.C., Lipman, P.W., and Zoback, M.L. eds., The Cordilleran Orogen, Geological Society of America, p. 0, doi:10.1130/DNAG-GNA- G3.107.

Salmon, E., 2006, Distribution of pre-Quaternary and Quaternary geologic units at the former terminus of the Cordilleran Ice Sheet: analysis of map realations north of Polson Montana: Graduate Student Theses, Dissertations, & Professional Papers, https://scholarworks.umt.edu/etd/8280.

Single-grain optical dating of Quaternary sediments: why aliquot size matters in luminescence dating - DULLER - 2008 - Boreas - Wiley Online Library, https://onlinelibrary.wiley.com/doi/abs/10.1111/j.1502-3885.2008.00051.x (accessed April 2023).

Smith, L.N., 2004, Late Pleistocene stratigraphy and implications for deglaciation and subglacial processes of the Flathead Lobe of the Cordilleran Ice Sheet, Flathead Valley, Montana, USA: Sedimentary Geology, v. 165, p. 295–332, doi: 10.1016/j.sedgeodoi: 10.1016/j.sedgeo.2003.11.013.

Smith, L., Blood, L., and Lafave, J., 2000, Quaternary geology, geomorphology, and hydrogeology of the upper Flathead River Valley area, Flathead County, Montana.

Smith, L., Sohbati, R., Buylaert, J.-P., Lian, O., Murray, A., and Jain, M., 2018, Timing of lake-level changes for a deep last-glacial Lake Missoula: optical dating of the Garden Gulch area, Montana, USA: Quaternary Science Reviews, v. 183, p. 23–35, doi: 10.1016/j.quascirevdoi: 10.1016/j.quascirev.2018.01.009.

Spencer, Joel & Spencer, Trevor. (2019). New Chronological Data on The Furthest Extent of The Southeastern Flathead Lobe of The Cordilleran Ice Sheet From Luminescence Studies Of Glacio-Deltaic And Moraine Deposits, Flathead Valley, Montana. 10.1130/abs/2019AM-340294.

Spencer, J., and Owen, L., 2004, Optically stimulated luminescence dating of Late Quaternary glaciogenic sediments in the upper Hunza Valley: Quaternary Science Reviews, v. 23, p. 175–191, doi:10.1016/S0277-3791(03)00220-8.

Stoffel, Keith L., "Glacial geology of the southern Flathead Valley Montana" (1980). Graduate Student Theses, Dissertations, & Professional Papers. 7426. https://scholarworks.umt.edu/etd/7426

Thrasher, I.M., Mauz, B., Chiverrell, R.C., and Lang, A., 2009, Luminescence dating of glaciofluvial deposits: A review: Earth-Science Reviews, v. 97, p. 133–146, doi: 10.1016/j.earscirevdoi: 10.1016/j.earscirev.2009.09.001.

Vuke, S.M., Porter, K.W., Lonn, J.D., and Lopez, D.A., 2007, Geologic Map of Montana: Montana Bureau of Mines and Geology Geologic Map 62-B, scale 1:500,000.

Wintle, A.G., and Murray, A.S., 2006, A review of quartz optically stimulated luminescence characteristics and their relevance in single-aliquot regeneration dating protocols: Radiation Measurements, v. 41, p. 369–391, doi: 10.1016/j.radmeas.2005.11.001